DMD Fast Forward. Published on January 9, 2023 as DOI: 10.1124/dmd.122.001096
This article has not been copyedited and formatted. The final version may differ from this version.

Absorption, Metabolism, and Excretion of Taselisib (GDC-0032), a Potent β-sparing PI3K Inhibitor, in Rats, Dogs, and Humans

Shuguang Ma[*, 1], Sungjoon Cho*, Srikumar Sahasranaman[2], Weiping Zhao, Jodie Pang, Xiao Ding, Brian Dean, Bin Wang[3], Jerry Y. Hsu[4], Joseph Ware[5], Laurent Salphati

Department of Drug Metabolism and Pharmacokinetics (SM, SC, WZ, JP, XD, BD, LS) and Department of Clinical Pharmacology (SS, JH, JW), Genentech, Inc., 1 DNA Way, South San Francisco, CA, 94080; XenoBiotic Laboratories (BW), Inc., 107 Morgan Lane, Plainsboro, NJ 08536

* Contributed equally

[1]Current affiliation: Pharmacokinetics and Drug Metabolism, Amgen, Inc., South San Francisco, CA

[2] Current affiliation: Clinical Pharmacology, BeiGene, San Mateo, CA

[3] Current affiliation: Ingredient Research, The Coca-Cola Company, Atlanta, GA

[4] Current affiliation: Clinical Development, ArriVent Biopharma, Burlingame, CA

[5] Current affiliation: Clinical Pharmacology, Seagen, South San Francisco, CA

DMD Fast Forward. Published on January 9, 2023 as DOI: 10.1124/dmd.122.001096
This article has not been copyedited and formatted. The final version may differ from this version.

Corresponding author:

Laurent Salphati, Pharm.D., Ph.D.

Drug Metabolism and Pharmacokinetics, Genentech, Inc., 1 DNA Way, South San Francisco, CA 94080. Phone: 650-467-1796. Email: salphati.laurent@gene.com

DMD Fast Forward. Published on January 9, 2023 as DOI: 10.1124/dmd.122.001096
This article has not been copyedited and formatted. The final version may differ from this version.

Running Title: Absorption, Metabolism, and Excretion of Taselisib

Text pages: 37

Table count: 4

Figure count: 11

Reference count: 28

Abstract: 249 words

Introduction: 437 words

Discussion: 1626 words

Abbreviations:

ABA, Absolute bioavailability; ADME, absorption, distribution, metabolism, and excretion; AMS, Accelerator mass spectrometry; AUC, area under the curve; BDC, Bile-duct cannulated; COMT, Catechol-O-Methyltransferase; F_a, fraction absorbed; F_e, fraction excreted; F_g, fraction escaping gut metabolism; F_h, fraction escaping hepatic metabolism; HMBC, Heteronuclear Multiple Bond Correlation; HMMT, histamine N-methyltransferase; HSQC, Heteronuclear Single Quantum Coherence; MS, Mass spectrometry; PI3K, Phosphoinositide 3-kinase; HPLC, high performance liquid chromatography; MetID, metabolite identification, NNMT, nicotinamide N-methyltransferase; SAM, S-adenosyl-L-methionine; TMT, thiol methyltransferase; TMPT, thiopurine methyltransferase;

DMD Fast Forward. Published on January 9, 2023 as DOI: 10.1124/dmd.122.001096
This article has not been copyedited and formatted. The final version may differ from this version.

Abstract

Taselisib (also known as GDC-0032) is a potent and selective phosphoinositide 3-kinase (PI3K) inhibitor that displays greater selectivity for mutant PI3Kα than wild-type PI3Kα. To better understand the ADME properties of taselisib, mass balance studies were conducted following single oral doses of [^{14}C]taselisib in rats, dogs, and humans. Absolute bioavailability (ABA) of taselisib in humans was determined by oral administration of taselisib at the therapeutic dose followed by iv dosing of [^{14}C]taselisib as a microtracer. The ABA in humans was 57.4%. Absorption of taselisib was rapid in rats and dogs and moderately slow in humans. The recovery of radioactivity in excreta was high (>96%) in the three species where feces was the major route of excretion. Taselisib was the major circulating component in the three species with no metabolite accounting for >10% of the total drug-derived material. The fraction absorbed (Fa) of taselisib was 35.9% in rats and 71.4% in dogs. In rats, absorbed drug underwent moderate to extensive metabolism and biliary excretion of taselisib was minor. In dog, biliary excretion and metabolism were major clearance pathways. In humans, 84.2% of the dose was recovered as the parent drug in excreta indicating that metabolism played a minor role in the drug's clearance. Major metabolism pathways were oxidation and amide hydrolysis in the three species while methylation was another prominent metabolism pathway in dogs. The site of methylation was identified on the triazole moiety. In vitro experiments characterized that the N-methylation was dog-specific and likely mediated by a thiol methyltransferase.

DMD Fast Forward. Published on January 9, 2023 as DOI: 10.1124/dmd.122.001096
This article has not been copyedited and formatted. The final version may differ from this version.

Significance Statement

This study provides a comprehensive description of the AME and pharmacokinetic properties of taselisib in preclinical species and humans. This study demonstrated the importance of oral bioavailability results for understanding taselisib's clearance pathways. The study also described the identification and characterization of a unique dog-specific N-methylation metabolite of taselisib and the enzyme mediating N-methylation in vitro.

DMD Fast Forward. Published on January 9, 2023 as DOI: 10.1124/dmd.122.001096
This article has not been copyedited and formatted. The final version may differ from this version.

Introduction

The phosphoinositide 3-kinase (PI3K) pathway is crucial for the growth, proliferation and survival of healthy and tumor cells. It is a key pathway that is activated by upstream receptor tyrosine kinases that are known to stimulate cancer cell proliferation, such as Human epidermal growth factor receptor 2 (HER2), epidermal growth factor receptor (EGFR), and insulin-like growth factor 1 receptor (IGF-1R). Activating mutations, as well as amplification, in the p110α subunit of PI3K have been identified in many tumor types (Shayesteh et al., 1999; Bachman et al., 2004; Massion et al., 2004; Samuels et al., 2004; Wu et al., 2005). These activating mutations have been shown to promote the growth and invasion in cancer cells that can be abrogated by PI3K inhibitors. The pathway can also be constitutively activated by the loss of the tumor suppressor phosphatase and tensin homolog (PTEN), a phosphatase that counteracts the kinase activity of PI3K, in many tumor types (Li et al., 1997; Steck et al., 1997). Further downstream, PI3K-pathway activity leads to the phosphorylation and activation of serine/threonine kinase Akt and mammalian target of rapamycin (mTOR). One of the most mutated oncogenes in hormone-receptor-positive (HR-positive) metastatic breast cancer (mBC) is PIK3CA, the gene encoding for the catalytic subunit of PI3K which is amplified in 37% and mutated in 9% of squamous lung cancers. As a result, small molecule inhibitors that target the PI3Ks have been actively pursued by pharmaceutical companies as potential treatments for various types of cancers (Shuttleworth et al., 2011).

Taselisib, 2-{3-[2-(1-isopropyl-3-methyl-1*H*-1,2−4-triazol-5-yl)-5,6-dihydrobenzo[f]imidazo[1,2-*d*][1,4]oxazepin-9-yl]-1*H*-pyrazol-1-yl}-2-methylpropanamide (GDC-0032, Figure 1A), is a potent inhibitor of PI3K that displays greater selectivity for mutant PI3Kα isoforms than wild-type PI3Kα in vitro (Ndubaku et al., 2013). It has demonstrated

DMD Fast Forward. Published on January 9, 2023 as DOI: 10.1124/dmd.122.001096
This article has not been copyedited and formatted. The final version may differ from this version.

activity in nonclinical models of PI3K-mutant tumor cells in vitro and in vivo and has been proven to be potent in nonclinical xenograft models of PI3K-mutant breast tumors. In preclinical studies, taselisib demonstrated promising pharmacokinetic properties, with low plasma clearance (CL) in mice, rats, and monkeys, and moderate CL in dogs relative to hepatic blood flow in these species (Ndubaku et al., 2013).

In order to better understand the absorption, metabolism, and excretion (AME) of taselisib in animals and humans, single oral dose studies using ^{14}C-labeled drug were conducted in rats, dogs (preclinical species used for toxicological studies), and humans. Absolute bioavailability was assessed using a microtracer approach in which a ^{14}C-labeled IV microdose was concomitantly administered at the T_{max} of an unlabeled therapeutic oral dose. Collectively, these data provided a comprehensive description of the AME and pharmacokinetic properties of taselisib in preclinical species and humans.

Materials and Methods

Chemicals and Reagents. [^{14}C]Taselisib (Figure 1A) was synthesized by Selcia (Essex, UK) with a specific activity of 55 mCi/mmol. It had a radiochemical purity 99.8% determined by HPLC coupled with in-line radio-detector. Unlabeled taselisib (chemical purity 98.4%) was synthesized at Genentech, Inc. (South San Francisco, CA). The internal standard for the quantitative LC-MS/MS assays of parent drug was the $^{13}C_6$ analog of taselisib. Acetonitrile (ACN) and ultrapure HPLC water were purchased from EMD Chemicals (Gibbstown, NJ). Deuterium oxide (>99% D) was obtained from Thermo Fisher Scientific (Bridgewater, NJ). Ammonium acetate solution (5.0 M) was purchased from Rockland (Gilbertsville, PA). Pico-Fluor 40 carbon-14 cocktail for liquid scintillation counting was from

DMD Fast Forward. Published on January 9, 2023 as DOI: 10.1124/dmd.122.001096
This article has not been copyedited and formatted. The final version may differ from this version.

PerkinElmer (Waltham, MA). All other reagents or materials used in these studies were purchased from Sigma-Aldrich (St. Louis, MO) unless otherwise stated. Hepatocytes (human, mouse, rat, dog and monkey) were purchased from BioreclamationIVT (Westbury, NY). Dog liver microsome (DLM) and dog liver cytosol (DLC) were purchased from Xenotech (Kansas City, KS). Recombinant dog nicotinamide N-methyltransferase (NNMT) was purchased from SignalChem (Richmond, Canada)

Mass Balance Studies of [^{14}C]Taselisib in Rats and Dogs. Rat and dog studies were performed at Covance (Madison, WI). Sprague-Dawley (SD) rats were purchased from Hilltop Lab Animals (Scottdale, PA). Beagle dogs were purchased from Covance Research Products (Kalamazoo, MI). Bile-duct cannulated (BDC) rats were provided from Hilltop Lab Animals and BDC dogs were prepared by Covance. Animals were fasted overnight before dosing of taselisib, and for 4h post-dose. BDC animals received bile salts replacement via infusion through the duodenal cannula. The oral formulation for animal studies was 0.5% methylcellulose and 0.2% Tween 80 in water (MCT).

Rats. Four groups of SD rats were administered a single oral dose at a target dose of 1 mg/kg (100 μCi/kg) of [^{14}C]taselisib. Group 1 (n=3 per sex) was used to evaluate excretion mass balance and metabolite profiles in urine and feces collected at pre-dose, 0-8 and 8-24 h post-dose, and at 24 h intervals up to 192 h post-dose. Group 2 included BDC animals (n=3 per sex) for absorption and biliary excretion determination. Bile and urine were collected from Group 2 animals at pre-dose, 0-8 and 8-24 h post-dose and at 24 h intervals up to 168 h post-dose. Group 3 (n=3 per sex) was designated for pharmacokinetic analysis. From these animals, blood (approximately 0.25 ml) was collected from the jugular vein at pre-dose and at 0.083, 0.25, 1, 3, 6, 12, 24, 48, 72 and 120 h post-dose and plasma was prepared. Group 4 (n=8 per sex) animals

DMD Fast Forward. Published on January 9, 2023 as DOI: 10.1124/dmd.122.001096
This article has not been copyedited and formatted. The final version may differ from this version.

were for profiling of circulating metabolites. One animal per sex was sacrificed via cardiac puncture and as much blood as possible was collected at pre-dose and 0.5, 1, 3, 6, 12 and 48 h post-dose to provide sufficient plasma for analysis.

Dogs. Male (n=2) and female (n=2) beagle dogs (Group 1) and BDC male beagle dogs (n=2) (Group 2) were administered a single oral dose of [^{14}C]taselisib at a target dose of 2 mg/kg (20 µCi/kg). Urine and feces were collected from animals in Groups 1 (bile duct-intact) and 2 (BDC) at pre-dose, 0–8 and 8–24 hours post-dose, and at 24 hour intervals up to 240 hours post-dose. Bile was collected from male BDC dogs in Group 2 at pre-dose, 0–8 and 8–24 h post-dose, and at 24 h intervals up to 168 hours post-dose. Blood samples were collected from animals in Group 1 and 2 at pre-dose and at 0.083, 0.25, 0.5, 1, 3, 6, 12, 24, 48, 72, 96, 120, 168 and 240 h post-dose. Blood samples were centrifuged to obtain plasma.

Human Absolute Bioavailability and Mass Balance Study. The clinical portion of this study was conducted by Covance Inc. (Madison, WI) as an open-label, non-randomized, single dose study to determine the absolute bioavailability, mass balance, routes of excretion, and metabolite profiling and identification of taselisib in humans. The study consisted of 2 arms (Arms A and B), where taselisib was administered as both a single oral and IV radiolabeled micro-tracer ([^{14}C]taselisib) dose (Arm A) and as a single radiolabeled ([^{14}C]taselisib) oral dose (Arm B). The study schemes of Arm A and Arm B are presented in Figure 1B. In both Arm A and B, dosing was preceded by an overnight fast (i.e., at least 8 hours) from food (not including water) and was followed by a fast from food (not including water) for at least 4 hours postdose following oral dose administration.

In the morning of Day 1, subjects in Arm A of the study (male, n=8) received a single 3 mg oral dose of taselisib (powder in capsule formulation) with 240 mL of water followed 4 hours later by

DMD Fast Forward. Published on January 9, 2023 as DOI: 10.1124/dmd.122.001096
This article has not been copyedited and formatted. The final version may differ from this version.

a single 3 μg IV dose of [^{14}C]taselisib containing approximately 200 nCi as a 2 mL manual IV push over 3 minutes. Subjects in Arm A were confined for 11 days from the time of Check-in (Day -1) until Study Completion on Day 11.

For Arm B, in the morning of Day 1, subjects in Arm B of the study (male, n=6) received a single 3-mg oral dose of [^{14}C]taselisib (powder in capsule formulation) containing approximately 200 μCi with 240 mL room temperature water. This radioactive dose was selected to ensure that low levels of metabolites would be detectable and was expected to lead to radiation exposure well below (~ 1% of) the recommended limits in humans, based on dosimetry calculations. Subjects in Arm B were confined from the time of Check-in (Day -1) for a minimum of 15 days and a maximum of 22 days, based on subjects meeting the study discharge criteria. Discharge criteria were (1) blood and plasma radioactivity reaches levels below the limit of quantification in 2 consecutive samples and (2) ≥90% of the dose is recovered OR ≤1% of the administered dose is excreted in urine and feces for 2 consecutive days.

Human Sample Collection. For Arm A, blood samples for PK analysis of taselisib were collected predose, and at 1, 2, 3, 4 (before start of manual IV push), 4 h and 1 min (i.e., 1 min into the manual IV push), 4 h and 3 min, 4 h and 15 min, 4.5, 5, 6, 8, 12, 24, 48, 72, 96, 120, 168 and 240 h post dose. For Arm B, blood samples for PK analysis and metabolite profiling in plasma were collected predose and at 1, 2, 3, 4, 6, 8, 12, 24, 36, 48, 72, 96, 120, 168, 240 and 336 h post dose. Urine was collected predose, and at 0 to 12 h, 12 to 24 h; and then at 24-h intervals until the subject was discharged from the clinical site. Fecal samples were collected predose; and at 24-h intervals until the subject was discharged from the clinical site.

Radioanalysis. The total radioactivity in blood, plasma, urine, and bile from rats and dogs was counted directly by liquid scintillation counters (LSC, PerkinElmer, Waltham, MA). The total

DMD Fast Forward. Published on January 9, 2023 as DOI: 10.1124/dmd.122.001096
This article has not been copyedited and formatted. The final version may differ from this version.

radioactivity in human blood and feces from Arm B was combusted in a biological sample oxidizer and evolved $^{14}CO_2$ was trapped and analyzed by LSC. The total radioactivity in human plasma and urine from Arm B was analyzed directly by LSC.

Concentrations of total [^{14}C] radioactivity and [^{14}C]taselisib in plasma from Arm A was determined using accelerator mass spectrometry (AMS), (Eckert & Ziegler Vitalea Science, Davis, CA) or high performance liquid chromatography (HPLC) fractionation followed by AMS analysis, respectively. For [^{14}C]taselisib measurement, samples were injected to Zorbax Eclipse XDB-C18 5µm 2.1x150 mm (Agilent Technologies, CA) after protein precipitation extraction of plasma. The mobile phases were 10 mM ammonium acetate (A) and ACN (B). The gradient started with 20% B and was held for 1 min, ramped up to 25% B in 7 min. The gradient was then ramped up to 95% B over 4 min and was held at 95% B for 2 min and ramped downed to 20% B in 1 min and held at 20% B for 5 min. The total run time was 20 min. The flow rate was 0.75 mL/min.

LC fractions corresponding to [^{14}C]taselisib were collected for AMS analysis. Samples were introduced into the AMS as solid elemental graphite after a two-stage process that involved oxidation to gaseous CO2 followed by reduction to graphite. The AMS instrument used was the BioMICADAS (PSI/ETH Zurich, Switzerland).

Extraction of Metabolites from Biological Samples.

Rat. Plasma samples collected from male and female rats in Group 4 at 0.5, 1, 3, 6, and 12 h post-dose were pooled by gender to generate single pooled samples using the trapezoidal AUC pooling method (Hop et al., 1998). Plasma samples were protein precipitated by adding ACN followed by vortex mixing, sonication, and centrifugation. The supernatant was separated and

DMD Fast Forward. Published on January 9, 2023 as DOI: 10.1124/dmd.122.001096
This article has not been copyedited and formatted. The final version may differ from this version.

the procedure was repeated. The combined supernatants were evaporated to dryness, and reconstituted with 10 mM ammonium acetate pH 5: ACN (4:1, v:v) for radio-profile analysis. Urine, feces, and bile samples were pooled from 0 to 48 h post-dose. Before injection to the LC column, urine and bile samples were centrifuged to remove solid matter. Pooled fecal homogenates were extracted with ACN. The supernatants were evaporated to dryness, and reconstituted with 10 mM ammonium acetate pH 5: ACN (4:1, v:v) for radio-profile analysis.

Dog. Plasma samples at pre-dose, and 0.083, 0.25, 0.5, 1, 3, 6, and 12 h post-dose were selected for metabolite profiling. These samples were pooled using the trapezoidal AUC pooling method (Hop et al., 1998). Three volumes of ACN were added to each pooled plasma sample. The samples were mixed by vortex, sonicated and centrifuged. The supernatants were transferred to a new set of tubes. The extraction procedure was repeated on the post-extraction solids following the same procedures. The supernatants from two extractions were combined, evaporated to near-dryness and reconstituted with water:ACN (2:1, v/v) for radio-profile analysis.

Urine, feces, and bile samples were pooled from 0 to 48 h, 0 to 48 h, and 0 to 24 h post-dose, respectively. Urine and bile samples from dogs were handled in a same way as to rat urine and bile samples. Pooled fecal homogenates were extracted with ACN, and the supernatants were evaporated to about two-thirds of the original sample weight (v/w) using a SpeedVac, and reconstituted with ACN for injection onto an HPLC column.

Human. Plasma samples at pre-dose, 1, 2, 3, 4, 6, 8, 12, 24, 36, 48, 72, and 96 h post-dose were pooled proportionally to PK area under the curve (AUC) separately for each subject (Hop et al., 1998). Three volumes of ACN were added to pooled plasma and the mixture was vortexed, sonicated and centrifuged. The supernatant was transferred to a new set of tubes. The extraction procedure was repeated on the post extraction solids following the same procedures. The

DMD Fast Forward. Published on January 9, 2023 as DOI: 10.1124/dmd.122.001096
This article has not been copyedited and formatted. The final version may differ from this version.

supernatants from two extractions were combined, evaporated to near-dryness using a SpeedVac concentrator, and reconstituted with H_2O:ACN (2:1, v:v) for radio-profile analysis.

Urine and feces samples were pooled from 0 to 144 h and 0 to the latest sampling time (i.e., 144, 168, 192 or 216 h) respectively. Before injection to the LC column, urine samples were centrifuged to remove solid matter. Pooled fecal homogenates were extracted with three volumes of ACN. The extraction was repeated on the post extraction solids following the same procedures. The supernatants from two extractions were evaporated to about two-thirds of the original sample weight (v/w) using a SpeedVac, and reconstituted with ACN for injection onto an HPLC column.

Metabolite Profiling. Liquid chromatography was performed with an Accela ultra performance liquid chromatography system comprised of a solvent pump with built-in degasser, temperature-controlled autosampler, and photodiode array detector (Thermo Scientific, San Jose, CA). The column used was an Eclipse XDB-C18, 4.6 x 150 mm, 5 µm (Agilent Technologies, Santa Clara, CA) and mobile phases of 10 mM ammonium acetate (pH=5) (mobile phase A) and ACN (mobile phase B) were used. The flow rate was 1 ml/min. The 60 min-HPLC gradient was as follows: mobile phase B was held at 0% for 5 min, increased to 5% at 15 min, to 20% at 15.1 min, to 25% at 40 min, to 95% at 50 min and held for 5 min, then decreased to 0% at 55.1 min and held for 5 min. The HPLC column effluent was split into radiodetector or fraction collector (0.75 mL/min) and mass spectrometer (0.25 mL/min).

For radio-profiling, the column effluent was directed to a fraction collector and collected on DeepWell LumaPlate-96 microplates (PerkinElmer) on the basis of time. Each fraction was collected for 0.22 minutes. The fractions were evaporated under vacuum and the plates were sealed with transparent TopSeal covers (PerkinElmer). Radioactivity in each well was measured

DMD Fast Forward. Published on January 9, 2023 as DOI: 10.1124/dmd.122.001096
This article has not been copyedited and formatted. The final version may differ from this version.

using a TopCount NXT scintillation and luminescence counter (PerkinElmer) for 5 minutes at 20°C. HPLC radio-chromatograms were reconstructed using the LSC import function in Laura evaluation software (LabLogic Systems, Tampa, FL). Radioactive peaks were integrated to calculate the distribution of sample radioactivity, and converted to the percentage of the dose by multiplying the distribution by the percentage of administered dose recovered in urine, feces, or bile.

Metabolite Identification. Mass spectrometric (MS) spectra were obtained with an LTQ-Orbitrap high resolution mass spectrometer operating in a positive ion mode with a heated electrospray ionization source from Thermo Fisher Scientific (San Jose, CA). The electrospray ion source voltage was 4.0 kV and heated capillary temperature was 300ºC. The scan-event cycle consisted of a full-scan mass spectrum at resolving power of 30,000 and the corresponding data-dependent scans were acquired at a resolving power of 7,500. Accurate mass measurements were performed using external calibration.

Taselisib Quantitation by LC-MS/MS in Human Plasma. For the determination of Taselisib concentrations in circulation in humans (both Arm A & B), plasma samples were processed with solid phase extraction and the resulting samples were injected to a Pursuit PFP column (50×2.0 mm, 3 µm particle size) (Varian, Lake Forest, CA). The LC-MS/MS system consisted of a Shimadzu LC-20 system (Shimadzu Inc., Columbia, MD) coupled with an API 5000 triple quadrupole mass spectrometer (AB Sciex, Foster City, CA). The mobile phases were water containing 0.1% formic acid (A) and ACN with 0.1% formic acid (B). The gradient started with 30% B and was ramped up to 40% B in 1.5 min. The gradient was then ramped down to 30% B over 0.1 min and was held at 30% B for 0.8 min. The total run time was 2.4 min. The flow rate was 0.5 mL/min. Taselisib and taselisib-d_6 were ionized using an atmospheric pressure chemical

DMD Fast Forward. Published on January 9, 2023 as DOI: 10.1124/dmd.122.001096
This article has not been copyedited and formatted. The final version may differ from this version.

ionization (APCI) source operating in the positive ionization mode. The quantitation of taselisib was performed using MRM transitions with 150 ms and 100 ms dwell times for taselisib and taselisib-d_6, respectively. Source temperature was 500 °C, declustering potential was 110 V and collision energy was 50 V for taselisib and 40 V for taselisib-d_6. The MRM transitions monitored were m/z 461.5 to m/z 334.2 for taselisib and m/z 467.5 to m/z 420.1 for taselisib-d_6. The method was validated over the calibration curve range 0.400–400 ng/mL (Ding et al., 2016).

PK Analysis. PK parameters of total radioactivity and parent drug (in humans only) were calculated by noncompartmental analysis using WinNonlin (version 5.2.1., Pharsight, Mountain View, CA).

Metabolite Isolation of M17 and Structure Characterization by NMR. Dog bile and feces samples across all animals and time intervals were pooled, respectively. Pooled bile sample was processed through solid-phase extraction (SPE) using Oasis® HLB 35cc cartridges, while pooled feces sample was extracted with methanol. The extracts were combined, concentrated, fractionated using SPE, then isolated by HPLC. Liquid chromatography was performed with a Waters® 2695 Separations Module (Milford, MA) and a Phenomenex Kinetex EVO C_{18}, 5 µm, 150 x 4.6 mm column (Torrance, CA). Mobile phases were 0.05% formic acid in water (mobile phase A) and ACN (mobile phase B). The flow rate was 1 ml/min. The 36 min-HPLC gradient was as follows: mobile phase B was held at 10% and increased to 40% at 20 min, to 100% at 21 min and held for 5 min, then decreased to 10% at 26.01 min and held for 10 min. The HPLC effluents were collected by time (10 sec/fraction) using a Foxy 200 fraction collector. The fractions from 15.5 to 16.2 min were combined, dried under a N2 stream, and further purified using an ion-exchange SPE cartridge (Waters Oasis® WCX 3cc) to yield M17 for NMR

DMD Fast Forward. Published on January 9, 2023 as DOI: 10.1124/dmd.122.001096
This article has not been copyedited and formatted. The final version may differ from this version.

analysis. Data were acquired on a Bruker 500 MHz NMR spectrometer using a 5 mm QNP probe (Billerica, MA).

H/D Exchange LC-MS. For hydrogen/deuterium (H/D) exchange LC-MS experiments to determine the methylation site of M17 in dog samples, deuterium oxide (> 99% D) was used as mobile phase A while all other chromatographic conditions remained the same as described previously and dog samples were analyzed.

In Vitro Experiments. Taselisib (10 μM) was incubated with human, mouse, rat, dog or monkey hepatocytes (approximately 1.5 million cells/mL) for 3 hours. The reactions were terminated by adding three volume ACN and centrifuged at 2000 x g for 15 min. The mixture was evaporated to dryness and reconstituted with 3:1 water to ACN and 10 uL for injection.

To determine the cellular fraction responsible for M17 generation, taselisib (10 μM) was incubated with 3 mg/mL of dog liver microsome (DLM) or dog liver cytosol (DLC) in 50 mM phosphate buffer (pH 7.4) containing 5 mM magnesium chloride and 1 mM SAM for 1 hour. The reactions were terminated by adding three volume ACN and centrifuged at 2000 g for 15 min. The mixture was evaporated to dryness and reconstituted with mixture of water/ACN (3:1) and injected onto LC-MS/MS.

For inhibition assays, taselisib (10 μM) was incubated with dog hepatocytes (cell concentration was approximately 1.5 million cells/mL) in the presence and absence of chemical inhibitors for methyltransferases. The final concentration of inhibitors were 50 μM amodiaquine (histamine N-methyltransferase, HNMT inhibitor), 5 μM tolcapone (catechol-O-methyltransferase, COMT inhibitor), 50 μM sulfasalazine (thiopurine methyltransferase, TMPT inhibitor), 1 mM 2,3-dichloromethylbenzylamine hydrochloride (thiol methyltransferase, TMT inhibitor) and 100 μM 1-methyl nicotinamide (nicotinamide N-methyltransferase, NNMT inhibitor) (Maw et al., 2018).

DMD Fast Forward. Published on January 9, 2023 as DOI: 10.1124/dmd.122.001096
This article has not been copyedited and formatted. The final version may differ from this version.

The reactions were terminated by adding three volumes of ACN containing 50 nM propranolol and centrifuged at 2000 *g* for 15 min. The mixture was evaporated to dryness and reconstituted with mixture of water/ACN (3:1) and injected onto LC-MS/MS.

Additional incubations with taselisib (10 µM) and 2 µg/mL of recombinant dog NNMT were conducted in 50 mM phosphate buffer (pH 7.4) containing 5 mM magnesium chloride and 1 mM SAM in the presence and absence of 5-amino-1-methylquinolin-1-ium iodide (20 µM, a NNMT inhibitor). As a positive control, nicotinamide, a known substrate of NNMT was incubated with NNMT. The mixture was preincubated for 5 min in water bath at 37°C, followed by the addition of 1 mM SAM to start the reaction. After 1 hour, the reactions were terminated by adding three volumes of ACN with 50 nM propranolol and centrifuged at 2000 *g* for 15 min. The mixture was evaporated to dryness and reconstituted with mixture of water/ACN (3:1) and injected onto LC-MS/MS.

Samples from in vitro experiments were analyzed using an LTQ-Orbitrap Velos mass spectrometer (Thermo Scientific) equipped with an Accela ultra performance liquid chromatography. For taselisib and methylation-related metabolites, liquid chromatography for was performed with a Kinetex 2.6 µm, XB-C18 100A 100x2.1 mm column (Phenomenex) and mobile phases of 10 mM ammonium acetate (pH 5) (mobile phase A) and ACN (mobile phase B). The flow rate was 0.4 ml/min. The 23 min-HPLC gradient was as follows: mobile phase B was held at 2% for 2 min, increased to 50% at 15 min, to 95% at 15.5 min and held for 2 min, then decreased to 2% at 18 min and held for 5 min.

For nicotineamide and 1-methyl nicotinamide, liquid chromatography was performed with a Synergi 2.5 µm, Polar RP 100A 100 x 2 mm column (Phenomenex) and mobile phases of 10 mM ammonium acetate (pH 5) (mobile phase A) and ACN (mobile phase B). The flow rate was

DMD Fast Forward. Published on January 9, 2023 as DOI: 10.1124/dmd.122.001096
This article has not been copyedited and formatted. The final version may differ from this version.

0.4 ml/min. The 15 min-HPLC gradient was as follows: mobile phase B was started at 1% and held for 9 min, increased to 95% at 9.1 min, and held at 95% for 2.4 min, then decreased to 1% at 11.6 min and held for 3.4 min.

DMD Fast Forward. Published on January 9, 2023 as DOI: 10.1124/dmd.122.001096
This article has not been copyedited and formatted. The final version may differ from this version.

RESULTS

Pharmacokinetics and Absolute Bioavailability of Taselisib in Humans. A summary of PK parameters following administration of 3 mg oral taselisib and 3 μg (200 nCi) IV [^{14}C]taselisib in Arm A is presented in Table 1. The concentration-time profiles for taselisib and [^{14}C]taselisib in plasma for Arm A are presented in Figure 2A. Following oral administration of 3 mg taselisib, the rate of absorption of taselisib was moderate with average T_{max} of 5.28 hours. After reaching C_{max}, taselisib plasma concentrations appeared to decline in a biphasic manner with a mean terminal half-life ($t_{1/2}$) of 40.9 hours. The mean CL/F and Vz/F values for taselisib in plasma were 9.81 L/hr and 567 L, respectively. Following IV administration of 3 μg (200 nCi) [^{14}C]taselisib, plasma radioactivity declined in parallel to the taselisib concentrations with a mean terminal ($t_{1/2}$) of 39.1 hours. The mean CL and Vz values for [^{14}C]taselisib in plasma were 5.28 L/hr and 294 L, respectively. The mean absolute bioavailability (F) of taselisib following oral administration was 57.4%.

Blood and Plasma Total Radioactivity in Rats, Dogs and Humans. Pharmacokinetic parameters of blood and plasma total radioactivity (TRA) in rats, dogs and humans, and plasma taselisib in humans are summarized in Table 2. The blood and plasma concentration-time profiles of TRA and plasma taselisib concentration-time profile in humans are shown in Figure 2B. Since concentration and pharmacokinetic data indicated that there were no apparent gender differences in rats and dogs, data from male and female animals were averaged.

In rats, C_{max} of blood and plasma TRA were 985 and 1857 ng-Eq/g, respectively. T_{max} was 0.4 h suggesting the absorption of taselisib was rapid. Both blood and plasma $t_{1/2}$ were 3.2 h. Mean blood:plasma concentration ratios, where calculable, ranged from 0.495 through 0.744 (data in

DMD Fast Forward. Published on January 9, 2023 as DOI: 10.1124/dmd.122.001096
This article has not been copyedited and formatted. The final version may differ from this version.

file) indicating minimal association of drug-derived radioactivity with the cellular component of blood.

In dogs, C_{max} of blood and plasma TRA were 426 and 415 ng-Eq/g, respectively. T_{max} was 1.5 h after dosing suggesting that taselisib was readily absorbed. Both blood and plasma $t_{1/2}$ were 2.5 h. The average blood to plasma concentration ratios ranged from 0.936 to 1.14 indicating that the radioactivity was not preferentially distributed to the cellular component of the blood in dogs.

In humans, T_{max} of TRA and taselisib in plasma were 5 and 5.5 hours respectively, suggesting moderate to slow absorption. After reaching C_{max}, plasma concentrations declined in a biphasic manner, with mean terminal $t_{1/2}$ values of approximately 42, 39, and 44 hours observed for taselisib in plasma, TRA in plasma, and TRA in blood, respectively. The mean blood/plasma ratio for total radioactivity was approximately 1.23 for $AUC_{0-\infty}$ indicating low association of radioactivity with red blood cells. The longer T_{max} observed in humans compared to rats and dogs was most likely due to the difference in formulation, with rats and dogs receiving a homogenous MCT suspension, and humans being administered a powder-in-capsule.

Excretion and Mass Balance. The cumulative recoveries of the administered radioactivity in urine, feces, and bile from rats, dogs and humans are shown in Table 3 and Figure 3.

Rat. Following a single oral dose of [^{14}C]taselisib, radioactivity was rapidly excreted and the excretion of radioactivity was nearly complete by 24 hours post-dose. There was no gender difference in excretion of radioactivity. The predominant route of elimination of [^{14}C]taselisib-derived radioactivity was via feces accounting for 94.2% and 100% of the administered dose through 192 hours post-dose in male and female rats, respectively. Urinary excretion of radioactivity accounted for 5.58% and 2.97% of the dose through 192 hours post-dose in male and female rats, respectively. Biliary excretion of radioactivity through 168 h post-dose in BDC

DMD Fast Forward. Published on January 9, 2023 as DOI: 10.1124/dmd.122.001096
This article has not been copyedited and formatted. The final version may differ from this version.

rats accounted for 19.9% and 22.5% of the dose in male and female rats, respectively. Urinary excretion of radioactivity in BDC rats was 17.6% and 11.8% of the dose in male and female rats, respectively. Biliary and urinary recoveries of the administered dose indicated that absorption of [^{14}C]taselisib was approximately 36%, suggesting low to moderate absorption of taselisib.

Dog. The excretion profiles in bile duct-intact male and female dogs were similar. Radioactivity was eliminated rapidly, with averages of 97% of the administered dose recovered by 48 hours post-dose. The predominant route of elimination was via feces which accounted for 94.1% and 96.1% of the dose in male and female dogs, respectively. Urinary excretion was minimal and accounted for 2.18% and 2.46% of the dose in male and female dogs, respectively. In BDC male dogs, the majority of the radioactivity (68.9% of the administered dose) was recovered in bile, suggesting that biliary excretion played a major role in the elimination of [^{14}C]taselisib. The urinary excretion in BDC dogs accounted for 2.53% of the administered dose. Biliary and urinary recoveries of the administered dose indicated that absorption of [^{14}C]taselisib was approximately 72% of the administered dose, suggesting high absorption of taselisib in dogs.

Humans. Most of the administered radioactivity was recovered in the first 144 h post-dose (90.6%). The overall mean recovery of radioactivity in urine and feces samples was 104% over the 360-h study. A mean of 88.6% of the dose was recovered in feces and 15.0% was recovered in urine through the last collection interval, suggesting that the predominant route of elimination was via feces.

Structural Characterization and Identification of Taselisib Metabolites. The metabolites identified in this study with molecular ions, major fragments and sources where the metabolites were detected are listed in Supplementary Table S1. Seventeen metabolites were identified in

rats, dogs or humans and structure elucidations were performed with LC-MS/MS. Structures of M17 was confirmed by H/D exchange LC-MS and NMR.

Circulating Metabolites of Taselisib in Rats, Dogs and Humans.

Representative HPLC radiochromatograms of pooled plasma from rats, dogs and humans are shown in Figure 4.

Rats. No gender-dependent differences in plasma metabolite profiles were observed in rats. Radio-profiles in pooled plasma from rats showed that taselisib accounted for 94.1% of sample radioactivity and M10 (hydroxylation) accounted for 5.03%.

Dog. No gender-dependent differences in plasma metabolite profiles were observed in dogs. Taselisib was the most abundant drug-related material in pooled plasma accounting for 88.6% of the total plasma sample radioactivity. Four minor metabolites were detected, which were M9 (amide hydrolysis), M10 (oxidation), M11 (oxidation) and M17 (methylation), accounting for 3.90%, 1.84%, 4.55% and 1.13% of the total plasma sample radioactivity, respectively. M14 (methylation and oxidation), M15 (hydrolysis and methylation), and M16 (methylation and oxidation) were of minor abundance and were only detected by mass spectrometry.

Human. Taselisib was the only detectable radioactive peak in the pooled 0-96 h plasma from all six subjects, indicating that taselisib was the predominant drug-derived material in the circulation. No metabolite was detected in circulation.

Metabolite Profiles of Taselisib in Urine, Feces, and Bile. Urine, feces, and bile collections were pooled to represent >90% of the total radioactivity in the corresponding excretion routes and profiled to determine the distribution of metabolites (Table 4).

Rat. Representative HPLC radiochromatograms of urine, feces and bile from rats are shown in Figure 5. Radio-analysis of rat urine showed one prominent metabolite, M10 (1.76% of

DMD Fast Forward. Published on January 9, 2023 as DOI: 10.1124/dmd.122.001096
This article has not been copyedited and formatted. The final version may differ from this version.

administered dose), and numerous minor radioactive peaks in addition to [^{14}C]taselisib, all of which accounted for less than 0.575% of administered dose. Radio-analysis of fecal samples showed that taselisib was the major radioactive component and accounted for 72.1% of administered dose. The most abundant metabolite was M10, accounting for 15.5% of administered dose. M5, M9 and M11 were also detected, accounting for 2.74, 2.39 and 1.78%, respectively. In bile samples from BDC rats, M9 was the most abundant metabolite and accounted for 7.13% of administered dose. Biliary excretion of [^{14}C]taselisib was minor and accounted for 4.9% of the administered dose. M10 was also observed in bile accounting 3.07% of the administered dose. Numerous minor metabolites were observed including M1, M2, M3, M4, M5, M6, M7, M11 and M12, all of which accounted for less than 1% of the administered dose. Major metabolism pathways in rats were oxidation (M10) and hydrolysis of amide (M9)

Dog. Representative HPLC radiochromatograms of urine, feces and bile from dogs are shown in Figure 6. In urine, taselisib represented only 0.259% of the administered dose. Four relatively abundant urinary metabolites (M17, M9, M10, and M11) were characterized, representing 0.222%, 0.516%, 0.258%, and 0.622% of the dose, respectively. Other minor metabolites included M14, M15, and M16, and accounted for less than 0.1% of the dose.

In fecal samples from bile duct-intact dog, unchanged taselisib represented 24.8% of the administered dose, indicating that taselisib was extensively metabolized in dogs. Methylation metabolite, M17 was the most abundant metabolite in feces and accounted for 29.5% of the dose. Other major fecal metabolites included M9, M10, M11 and M16 representing 15.7%, 6.10%, 7.10% and 11.2%, of the dose, respectively. M14 and M15 were also detected, but were less than 0.5% of the dose. Methylation related metabolites (M14-M17) in feces together accounted for 41.4% of the dose, suggesting methylation was a major metabolism pathway.

DMD Fast Forward. Published on January 9, 2023 as DOI: 10.1124/dmd.122.001096
This article has not been copyedited and formatted. The final version may differ from this version.

In dog bile, taselisib accounted for 32.1% of the administered dose indicating that biliary secretion of unchanged drug was a major clearance pathway in dogs. The major metabolites in bile were M17 and M9, accounting for 18.1% and 9.08% of the dose, respectively. Other minor metabolites included M10, M11 and M16, which represented 1.89%, 4.79% and 2.95% of the administered radioactivity, respectively. Major metabolism pathways in dogs were methylation (M17), oxidation (M10, M11) and hydrolysis of amide (M9)

Human. Representative HPLC radiochromatograms of urine and feces from humans are shown in Figure 7. In urine, unchanged taselisib was the most abundant drug derived material and accounted for 12.3% of the dose. Three urinary metabolites (M9, M10, and M11) were detected accounting for 0.825%, 0.697% and 1.23% of the dose, respectively.

In fecal samples, unchanged taselisib was the most abundant component and represented 71.9% of the dose. M9 was the major metabolite in feces and accounted for 8.55% of the dose. Other fecal metabolites included M5, M6, M10 and M11, representing 2.65%, 1.44%, 0.868%, and 1.42% of the dose, respectively. Major metabolism pathways in humans were hydrolysis of amide (M9) and oxidation (M5, M6, M11).

Structure Characterization of M17 by H/D Exchange LC-MS and NMR

H/D exchange LC-MS experiments were performed to facilitate the structural characterization of the methylation metabolites of taselisib. The molecular ion of taselisib was observed at *m/z* 464.2596 following H/D exchange, which was 3 Da higher than that observed with non-deuterated mobile phases (data in file). The 3-Da mass increase for $[M + H]^+$ of taselisib is consistent with the exchange of two hydrogen atoms at the amide and the ionizing proton in $[M + H]^+$ with deuteriums. The molecular ion of M17 in deuterated solvent was detected at *m/z* 477.2692, which was 2 Da higher than that detected in non-deuterated mobile phases,

DMD Fast Forward. Published on January 9, 2023 as DOI: 10.1124/dmd.122.001096
This article has not been copyedited and formatted. The final version may differ from this version.

corresponding to the exchange of two hydrogen atoms at the amide with deuteriums. This result indicated that M17 does not require an ionizing proton, suggesting that the metabolite most likely contains a quaternary ammonium cation. Therefore, methylation had probably occurred on the nitrogen of triazole, imidazole or pyrazole ring. Similarly, the molecular ions of M14, M15 and M16 were observed at *m/z* 494.2712, *m/z* 477.2480, and *m/z* 494.2712, which were 3 Da, 1 Da, and 3 Da higher than those observed with non-deuterated mobile phases, respectively and suggested that methylation on those metabolites also likely occurred on the nitrogen of triazole, imidazole or pyrazole ring to form quaternary ammonium cations.

M17 was isolated and purified from dog bile and feces samples for definitive structure characterization using NMR. 1D (^{1}H) and 2D (HSQC and HMBC) NMR techniques were performed to elucidate the structure of M17. Likewise, the NMR data of taselisib were also obtained for comparison purpose. ^{1}H and ^{13}C NMR assignments of taselisib and M17 are summarized in Supplementary Table S2.

M17 has been characterized as an N-methyl metabolite. Proton and carbon chemical shifts of the additional methyl group of M17 (δH 3.95, δC 33.6, Supplementary Table S2) confirmed the presence of an N-methyl moiety. Key heteronuclear multiple bond correlation spectroscopy (HMBC) spectrum and correlations of M17 are depicted in Figure 8 (HSQC data are in file). HMBC correlations from H3-32 to C-23 and C-26 were observed, indicating the methylation occurred on the N-27 of the triazole moiety.

In Vitro Characterization of Enzymes Involved in Methylation of Taselisib in Dogs. In vitro experiments were conducted to determine the enzymes involved in the methylation of taselisib to M17. Hepatocytes from 5 species (human, mouse, rat, dog and monkey) were incubated with taselisib and only dog hepatocytes generated M17 (Figure 9A). This was consistent with in vivo

DMD Fast Forward. Published on January 9, 2023 as DOI: 10.1124/dmd.122.001096
This article has not been copyedited and formatted. The final version may differ from this version.

data showing that M17 was only observed in dogs, not in rats or humans. Both dog liver microsomes (DLM) and dog liver cytosols (DLC) were able to generate M17 from taselisib (Figure 9B), suggesting that multiple methyltransferases located in DLC or DLM were involved in the methylation of taselisib. In dog hepatocytes incubated with various methyltransferase inhibitors, DCMB significantly inhibited the formation of M17 (~ 98%) while others showed minimal or moderate (<30%) inhibition activity. Methylation-related metabolites M15 and M16 showed similar trend (Supplementary Figure S1) while M14 was not observed in dog hepatocytes. Recombinant dog NNMT was incubated with taselisib which showed minimal generation of M17 while it significantly methylated nicotinamide (a known substrate of NNMT) (Supplementary Figure S1C) confirming that NNMT was likely not involved in the methylation of taselisib.

DMD Fast Forward. Published on January 9, 2023 as DOI: 10.1124/dmd.122.001096
This article has not been copyedited and formatted. The final version may differ from this version.

Discussion

In the current study, the absorption, metabolism, and excretion of taselisib were characterized after a single oral dose in rats, dogs and humans.

In humans, the ABA of taselisib following a single oral dose of 3 mg taselisib as powder-in-capsule (PIC) was determined to be 57.4%. A relative BA study conducted later showed that the exposure obtained with the final tablet formulation was ~1.5-fold greater than that achieved with the PIC formulation (Faber et al., 2016). No further ABA study was performed with the tablet.

The study design with i.v. microtracer had numerous benefits. The number of healthy volunteers could be reduced and no wash-out period was needed in contrast to traditional absolute bioavailability studies. Since i.v microtracer was given at the T_{max} of orally administered taselisib in which the body was already exposed to the drug at the therapeutic dose, the possibility of non-linear PK of i.v microtracer was eliminated. This allows for comparison of the oral and IV doses when there are therapeutically relevant concentrations of drug systemically available. Additionally, simultaneous dosing resulted in less variability in the absolute bioavailability estimate, and ensured the systemic clearance was consistent for the IV and oral doses. A stable isotope labeled (SIL) microtracer with LC-MS/MS analysis would be a good alternative approach for ABA (Ma and Chowdhury, 2016). However, because the LC-MS/MS method could not achieve the required sensitivity at low pg/mL and the synthesis of another stable-labeled drug for IV microtracer presented technical difficulties, this approach was not used for this study.

Whole blood and plasma total radioactivity data suggested that all three species showed minimal association of drug-derived radioactivity with the cellular component of blood. The $t_{1/2}$ of TRA was comparable in rats and dogs, while that in humans was markedly longer, in agreement with

DMD Fast Forward. Published on January 9, 2023 as DOI: 10.1124/dmd.122.001096
This article has not been copyedited and formatted. The final version may differ from this version.

the slower excretion of total radioactivity compared to rats and dogs (Figure 4). This long $t_{1/2}$ in humans was underpredicted by the non-clinical data and PBPK modeling, mainly due to an overprediction of CL, as previously described (Heffron et al., 2022). Even though humans showed long $t_{1/2}$ of TRA, retention of radioactivity in the body was expected to be minimal based on the good mass balance achieved (almost 100% of the dose excreted in urine and feces) and the marginal contribution of AUC from the β-phase (i.e., terminal phase) to the total AUC (Table 1). Plasma TRA and taselisib concentrations in humans were almost identical (Figure 3C), which is consistent with minimal circulating metabolites detected in plasma (Figure 5).

The fraction absorbed (Fa) of taselisib was moderate in rats (35.9%) and high in dogs (71.4%) based on the sum of % dose excreted in the bile (Table 3) and urine in BDC animals. The fraction absorbed in humans (Fa) following oral dose could not be determined from this study since the parent drug recovered in feces (88.6% of the administrated dose) could come from the unabsorbed drug, biliary excretion of the absorbed drug, or both. Instead, we estimated Fa by the following calculations: Results from the ABA study indicated that the average bioavailability (F) of taselisib in humans was 0.574. According to mass balance and MetID results, 12.3% of dose in urine was unchanged taselisib ($f_{e,urine}$=0.123) and plasma renal CL was calculated to be 1.13 L/h ([$CL_{r,\,p} = (fe/F)*CL_{iv}$]. Therefore, hepatic plasma clearance ($CL_{h,\,p}$) was 4.15 L/hr (CL_{iv}-$CL_{r,p}$) and hepatic blood clearance ($CL_{h,b}$) was 3.37 L/h ($CL_{h,b} = CL_{h,\,p}/(C_b/C_p)$. Accordingly, F_h was estimated to be 0.961 ($F_h = 1 - CL_{h,b}/Q_h$) and hence, fraction absorbed (Fa) in humans was estimated to be at least 0.597 ($Fa = F/(F_h*F_g)$ assuming F_g was approximately 1. The estimated Fa was within the ranges of Fa values observed in rats and dogs. Fa of 0.597 suggested that unabsorbed fraction of taselisib was 0.403. Therefore approximately 32% of the dose as parent in feces was from biliary excretion ($F_{e,bile}$= fraction of unchanged parent excreted in feces – fraction

DMD Fast Forward. Published on January 9, 2023 as DOI: 10.1124/dmd.122.001096
This article has not been copyedited and formatted. The final version may differ from this version.

of unabsorbed parent = 0.719-0.403=0.316). Total metabolites in excreta represented 17.7% of dose. Therefore, f_m (fraction metabolized) was estimated to be 0.296 (0.177/Fa). The proposed disposition of taselisib after oral administration in humans based on these calculations is summarized in Figure 10. The estimation of the various fractions available (Fa, Fh) and the insight gained into the clearance pathways ($f_{e,bile}$ and f_m) relied on the determination of the oral bioavailability. This further emphasizes the importance of ABA studies in providing key information for the understanding of the disposition and clearance of orally administered compounds, such as taselisib.

In dogs, humans, and to a much lesser extent in rats, biliary elimination of unchanged taselisib was observed or estimated. This excretion was most likely mediated by P-glycoprotein and/or BCRP, since this compound is a substrate of both transporters (Pang et al., 2014) and studies in Pgp/BCRP knock-out mice and rats confirmed the prominent roles these transporters play in the biliary elimination of taselisib (Salphati, 2018). In addition, in a clinical DDI study, itraconazole co-administration led to 1.5-fold increase in the AUC of taselisib (Sahasranaman et al., 2015), which could be explained by inhibition of CYP3A4. However, considering that taselisib undergoes very limited metabolism, it is possible also that the higher exposure observed resulted from the inhibition of Pgp and/or BCRP by itraconazole. Taken together, these data suggest that the elimination of taselisisb in the bile is mediated by Pgp and/or BCRP in preclinical species and humans.

Proposed metabolic pathways of taselisib in rats, dogs and humans are presented in Figure 11. In rats, absorbed [^{14}C]taselisib underwent moderate to extensive metabolism and major metabolic pathways were hydrolysis to produce M9 and hydroxylation to produce M10.

DMD Fast Forward. Published on January 9, 2023 as DOI: 10.1124/dmd.122.001096
This article has not been copyedited and formatted. The final version may differ from this version.

In dogs, approximately 25% of the administered dose was recovered as the parent drug in urine and feces from the bile duct−intact dogs, indicating that taselisib was extensively metabolized. The major metabolic pathways included methylation, amide hydrolysis, oxidation, and the combination of oxidation and methylation. Methylation was only observed in dogs. Interestingly, percentage dose of M10 and M11 were higher in feces than that in bile in both rats and dogs suggesting that M10 and M11 could be also generated in the intestine or secreted directly from the systemic circulation into the intestine.

In contrast to rats and dogs, approximately 84.2% of the dose was recovered as the parent drug in humans, indicating that taselisib was mainly cleared as unchanged drug in urine and feces. Metabolism played a relatively minor role in the drug's clearance in humans. Major biotransformation pathway were amide hydrolysis and oxidation. The overall turnover of taselisib in vitro was very low. The hydrolytic metabolite M9 was barely detected, at the limit of quantitation, in hepatocyte incubations. These conditions did not allow us to study and identify the enzymes involved in the formation of M9.

Mass balance studies suggested that dogs exclusively produced N-methylation metabolites and in vitro hepatocytes experiments also confirmed that N-methylation was dog-specific. Species differences in N-methylation activity of pyridine were reported in vivo (D'Souza et al., 1980; Damani et al., 1982) and dog-specific N-methylation activities were also reported. Leeson et al. reported the N-methylation of oxprenolol in beagle dogs (Leeson et al., 1973) while Walle et al. reported a dog-specific N-methylation of N-demethylated metabolites of propranolol, alprenolol and oxprenolol (Walle et al., 1981). N-methylation and quaternization have been reported in a few nitrogen-containing heterocycles similar to N-methylation of taselisib (Damani and Case, 1984). For example, N-methylation of pyridine ring such as N-methylnicotine, N-

DMD Fast Forward. Published on January 9, 2023 as DOI: 10.1124/dmd.122.001096
This article has not been copyedited and formatted. The final version may differ from this version.

methylcotinine, ethionamide and N-methylation of the thiazole ring of anticonvulsant drug, chlormethiazole were reported (Damani and Case, 1984). To our knowledge, N-methylation of taselisib is the first example of N-methylation on triazole ring, which expands our knowledge about the chemical moieties potentially undergoing N-methylation.

There are a wide range of methyltransferase reported to mediate xenobiotic metabolisms and their cellular locations are cytosol or microsomes (Jancova et al., 2010). In vitro experiment showed that both dog liver cytosol and microsomes could mediate N-methylation of taselisib suggesting that multiple methyltransferases were involved in that reaction. Several methyltransferase inhibitors were tested and 2,3-dichloromethylbenzylamine (DCMB) significantly inhibited the methylation of taselisib (98%). DCMB is a thiol methyltransferase (TMT) inhibitor (Maw et al., 2018) . TMT is located mainly in microsomes (Kazui et al., 2014) but several studies showed that TMT activity was also detected in cytosol (Glauser et al., 1992; Liu et al., 2015; Maw et al., 2018). Although TMT is widely known to mediate S-methylation of a wide range of compounds (Obach et al., 2012; Kazui et al., 2014; Liu et al., 2015), N-methylation activity of TMT was also reported (Maw et al., 2018). Therefore, TMT might play a role in the methylation of taselisib in dogs though, this study cannot rule out that other methyltransferases might also be involved in the methylation of taselisib because DCMB might also inhibit other methyltransferases in dogs. The role of another N-methyltransferase, NNMT, on the N-methylation of taselisib was investigated using the recombinant dog enzyme. The data suggested that dog NNMT played a minor role, which was consistent with the minimal effect of the NNMT inhibitor 1-methyl nicotinamide, on taselisib methylation. It is worth noting though, that the specificity of 1-methyl nicotinamide for the dog enzyme is not as established as it is for the human NNMT.

DMD Fast Forward. Published on January 9, 2023 as DOI: 10.1124/dmd.122.001096
This article has not been copyedited and formatted. The final version may differ from this version.

In summary, this study comprehensively characterized the absorption, metabolism and excretion of taselisib in rats, dogs and humans. Absolute bioavailability of taselisib was also determined in humans. Overall, mass balance of taselisib was similar in the three species where fecal excretion was the major route of excretion. Taselisib was the major circulating component with minor metabolites in all three species. Major metabolism pathways were oxidation and amide hydrolysis in the three species while methylation was also a major metabolism pathway in dogs. Structures of dog-specific methylation metabolites and enzymes potentially mediating methylation were characterized.

DMD Fast Forward. Published on January 9, 2023 as DOI: 10.1124/dmd.122.001096
This article has not been copyedited and formatted. The final version may differ from this version.

Acknowledgement

The authors wish to thank the patients for enrolling in this study and taking valuable time away from their personal lives to advance science. We also wish to thank all principal investigators and their staff for the conduct of the clinical study. Their support is gratefully acknowledged.

Author Contributions

Participated in research design: Ma, Cho, Dean, Salphati

Conducted experiments: Ma, Cho, Zhao, Ding

Performed data analysis: Ma, Cho, Sahasranaman, Zhao, Pang, Ding, Dean, Hsu, Ware, Salphati

Wrote or contributed to the writing of the manuscript: Ma, Cho, Zhao, Dean, Salphati

Footnotes:

Funding

This work received no external funding.

Conflict of interest

The authors were employees of Genentech, Inc. or F. Hoffmann-La Roche Ltd when this work was completed

DMD Fast Forward. Published on January 9, 2023 as DOI: 10.1124/dmd.122.001096
This article has not been copyedited and formatted. The final version may differ from this version.

REFERENCES

Bachman KE, Argani P, Samuels Y, Silliman N, Ptak J, Szabo S, Konishi H, Karakas B, Blair BG, Lin C, Peters BA, Velculescu VE, and Park BH (2004) The PIK3CA gene is mutated with high frequency in human breast cancers. *Cancer biology & therapy* 3:772-775.

D'Souza J, Caldwell J, and Smith RL (1980) Species variations in the N-methylation and quaternization of [14C]pyridine. *Xenobiotica* 10:151-157.

Damani L and Case D (1984) Metabolism of heterocycles.

Damani LA, Crooks PA, Shaker MS, Caldwell J, D'Souza J, and Smith RL (1982) Species differences in the metabolic C- and N-oxidation , and N-methylation of [14C]pyridine in vivo. *Xenobiotica* 12:527-534.

Ding X, Faber K, Shi Y, McKnight J, Dorshorst D, Ware JA, and Dean B (2016) Validation and determination of taselisib, a beta-sparing phosphoinositide 3-kinase (PI3K) inhibitor, in human plasma by LC-MS/MS. *J Pharm Biomed Anal* 126:117-123.

Faber KP, Borin MT, Cheeti S, Fraczkiewicz G, Nelson E, Ran Y, Dresser MJ, Graham RA, Sahasranaman S, Hsu J, Ware JA, and Morrissey KM (2016) Impact of formulation and food on taselisib (GDC-0032) bioavailability: powder-in-capsule formulation represents unique drug development challenge. *Clinical Pharmacology & Therapeutics* Volume 99:Poster number: PI-067.

Glauser TA, Kerremans AL, and Weinshilboum RM (1992) Human hepatic microsomal thiol methyltransferase. Assay conditions, biochemical properties, and correlation studies. *Drug metabolism and disposition: the biological fate of chemicals* **20:**247-255.

Heffron TP, Salphati L, and Staben ST (2022) Discovery of Taselisib (GDC-0032), in: *Contemporary Accounts in Drug Discovery and Development*, pp 145-156.

Hop CE, Wang Z, Chen Q, and Kwei G (1998) Plasma-pooling methods to increase throughput for in vivo pharmacokinetic screening. *Journal of pharmaceutical sciences* 87:901-903.

Jancova P, Anzenbacher P, and Anzenbacherova E (2010) Phase II drug metabolizing enzymes. *Biomedical papers of the Medical Faculty of the University Palacky, Olomouc, Czechoslovakia* 154:103-116.

Kazui M, Hagihara K, Izumi T, Ikeda T, and Kurihara A (2014) Hepatic microsomal thiol methyltransferase is involved in stereoselective methylation of pharmacologically active metabolite of prasugrel. *Drug metabolism and disposition: the biological fate of chemicals* **4**2:1138-1145.

Leeson GA, Garteiz DA, Knapp WC, and Wright GJ (1973) N-methylation, a newly identified pathway in the dog for the metabolism of oxprenolol, a beta-receptor blocking agent. *Drug metabolism and disposition: the biological fate of chemicals* 1:565-568.

Li J, Yen C, Liaw D, Podsypanina K, Bose S, Wang SI, Puc J, Miliaresis C, Rodgers L, McCombie R, Bigner SH, Giovanella BC, Ittmann M, Tycko B, Hibshoosh H, Wigler MH, and Parsons R (1997) PTEN, a putative protein tyrosine phosphatase gene mutated in human brain, breast, and prostate cancer. *Science* 275:1943-1947.

Liu C, Chen Z, Zhong K, Li L, Zhu W, Chen X, and Zhong D (2015) Human Liver Cytochrome P450 Enzymes and Microsomal Thiol Methyltransferase Are Involved in the Stereoselective Formation and Methylation of the Pharmacologically Active Metabolite

of Clopidogrel. *Drug metabolism and disposition: the biological fate of chemicals* 43**:**1632-1641.

Ma S and Chowdhury SK (2016) The use of stable isotope-labeled drug as microtracers with conventional LC-MS/MS to support human absolute bioavailability studies: are we there yet? *Bioanalysis* 8:731-733.

Massion PP, Taflan PM, Shyr Y, Rahman SM, Yildiz P, Shakthour B, Edgerton ME, Ninan M, Andersen JJ, and Gonzalez AL (2004) Early involvement of the phosphatidylinositol 3-kinase/Akt pathway in lung cancer progression. *American journal of respiratory and critical care medicine* 170**:**1088-1094.

Maw HH, Zeng X, Campbell S, Taub ME, and Teitelbaum AM (2018) N-Methylation of BI 187004 by Thiol S-Methyltransferase. *Drug metabolism and disposition: the biological fate of chemicals* 46**:**770-778.

Ndubaku CO, Heffron TP, Staben ST, Baumgardner M, Blaquiere N, Bradley E, Bull R, Do S, Dotson J, Dudley D, Edgar KA, Friedman LS, Goldsmith R, Heald RA, Kolesnikov A, Lee L, Lewis C, Nannini M, Nonomiya J, Pang J, Price S, Prior WW, Salphati L, Sideris S, Wallin JJ, Wang L, Wei B, Sampath D, and Olivero AG (2013) Discovery of 2-{3-[2-(1-isopropyl-3-methyl-1H-1,2-4-triazol-5-yl)-5,6-dihydrobenzo[f]imidazo[1 ,2-d][1,4]oxazepin-9-yl]-1H-pyrazol-1-yl}-2-methylpropanamide (GDC-0032): a beta-sparing phosphoinositide 3-kinase inhibitor with high unbound exposure and robust in vivo antitumor activity. *Journal of medicinal chemistry* 56:4597-4610.

Obach RS, Prakash C, and Kamel AM (2012) Reduction and methylation of ziprasidone by glutathione, aldehyde oxidase, and thiol S-methyltransferase in humans: an in vitro study. *Xenobiotica* 42:1049-1057.

Pang J, Baumgardner M, Cheong J, Edgar K, Heffron TP, Le H, Ndubaku O, Olivero AG, Plise EG, Staben ST, Wallin J, Wong S, Zhang X, and Salphati L (2014) Preclinical evaluation of the ß isoform-sparing PI3K inhibitor GDC-0032 and prediction of its human pharmacokinetics. *Drug metabolism reviews* 45 Suppl 1:219.

Sahasranaman S, Graham RA, Salphati L, Hsu J, Lu X, Gates M, Amin D, Bradford D, Dresser M, and Ware J (2015) Assessment of pharmacokinetic interaction between the PI3K inhibitor taselisib (GDC-0032) and a strong CYP3A4 inducer or inhibitor. *Clinical Pharmacology & Therapeutics* Volume 97:Poster number: PII-073.

Salphati L (2018) Interaction of The PI3Kinase Inhibitor Taselisib with Efflux Transporters: In Vivo and In Vitro Investigations. *Oral presentation at SMi ADMET Conference, London*.

Samuels Y, Wang Z, Bardelli A, Silliman N, Ptak J, Szabo S, Yan H, Gazdar A, Powell SM, Riggins GJ, Willson JK, Markowitz S, Kinzler KW, Vogelstein B, and Velculescu VE (2004) High frequency of mutations of the PIK3CA gene in human cancers. *Science* 304**:**554.

Shayesteh L, Lu Y, Kuo WL, Baldocchi R, Godfrey T, Collins C, Pinkel D, Powell B, Mills GB, and Gray JW (1999) PIK3CA is implicated as an oncogene in ovarian cancer. *Nature genetics* 21**:**99-102.

Shuttleworth SJ, Silva FA, Cecil AR, Tomassi CD, Hill TJ, Raynaud FI, Clarke PA, and Workman P (2011) Progress in the preclinical discovery and clinical development of class I and dual class I/IV phosphoinositide 3-kinase (PI3K) inhibitors. *Current medicinal chemistry* 18**:**2686-2714.

Steck PA, Pershouse MA, Jasser SA, Yung WK, Lin H, Ligon AH, Langford LA, Baumgard ML, Hattier T, Davis T, Frye C, Hu R, Swedlund B, Teng DH, and Tavtigian SV (1997)

Identification of a candidate tumour suppressor gene, MMAC1, at chromosome 10q23.3 that is mutated in multiple advanced cancers. *Nature genetics* 15**:**356-362.

Walle UK, Wilson MJ, and Walle T (1981) Propranolol, alprenolol and oxprenolol metabolism in the dog. Identification of N-methylated metabolites. *Biomedical mass spectrometry* **8:**78-84.

Wu G, Xing M, Mambo E, Huang X, Liu J, Guo Z, Chatterjee A, Goldenberg D, Gollin SM, Sukumar S, Trink B, and Sidransky D (2005) Somatic mutation and gain of copy number of PIK3CA in human breast cancer. *Breast cancer research : BCR* **7:**R609-616.

Table 1. Pharmacokinetic parameters in plasma for taselisib and [^{14}C]taselisib in humans after oral administration of taselisib (3 mg) followed by i.v administration of [^{14}C]taselisib (3 µg, 200 nCi) 4 h later (Arm A).

	Dose	C_{max} (ng eq/g)[a]	T_{max} (h)	$t_{1/2}$ (h)	AUC_{0-t} (ng eq*h/g)[b]	$AUC_{0-\infty}$ (ng eq*h/g)[b]	CL/F (L/h)[f]	Vz/F (L)[c,f]	$AUC_{0-\infty}$/Dose (ng*h/mL/mg)	F
Oral (Taselisib)	3 mg	6.96 (3.01)	5.28 (1.23)	40.9 (6.69)	334 (116)	342 (116)	9.81 (3.76)	567 (187)	114 (38.6)	0.574 (0.128)
IV ([^{14}C]Taselisib	3 µg (200 nCi)	47.3 (24.4)	0.05 (0.005)	39.1 (6.17)	574 (131)	589 (131)	5.28 (0.996)	294 (54.1)	196 (43.7)[d]	NA

AUC_{0-t}: area under the concentration-time curve from hour 0 to the last measurable concentration;
$AUC_{0-\infty}$: area under the concentration-time curve from hour 0 extrapolated to infinity.
Data are expressed as mean (SD).
[a] Units for [^{14}C]taselisib are pg equivalents/mL.
[b] Units for [^{14}C]taselisib are pg equivalents*hr/mL.
[c] Vz: volume of distribution during terminal phase.
[d] Units for [^{14}C]taselisib are pg equivalents*hr/mL/µg.
[f] CL and Vz for [^{14}C]taselisib.

Table 2. Pharmacokinetic parameters in blood, plasma total radioactivity (TRA) and plasma taselisib (only humans) in rats, dogs and humans after oral administration of [^{14}C]taselisib

	Dose[c]	Matix	Analyte	C_{max} (ng eq/g)	T_{max} (h)	$t_{1/2}$ (h)	AUC_{0-t} (ng eq*h/g)	$AUC_{0-\infty}$ (ng eq*h/g)
Rat[a]	1	Blood	TRA	985 (225)	0.4 (0.3)	3.2 (0.3)	6673 (839)	6718 (847)
		Plasma	TRA	1857 (409)	0.4 (0.3)	3.2 (0.2)	11833 (1385)	11900 (1389)
Dog[b]	2	Blood	TRA	426 (68)	1.5 (1.0)	2.5 (0.1)	2185 (352)	2293 (388)
		Plasma	TRA	415 (84)	1.4 (1.1)	2.5 (0.02)	2138 (436)	2240 (465)
Human (Arm B)	3	Blood	TRA	7.74 (2.61)	5.5 (1.8)	44 (4.2)	411 (114)	492 (127)
		Plasma	TRA	7.14 (2.39)	5.0 (2.0)	39 (6.2)	352 (117)	410 (130)
		Plasma	Taselisib	6.92 (2.51)	5.5 (1.8)	42 (4.5)	404 (114)	414 (115)

AUC_{0-t}: area under the concentration-time curve from hour 0 to the last measurable concentration;
$AUC_{0-\infty}$: area under the concentration-time curve from hour 0 extrapolated to infinity.
Data are expressed as mean (SD).
[a] Data from male (n=3) and female (n=3) rats were combined.
[b] Data from male (n=2) and female (n=2) dogs were combined.
[c] Dose units are mg/kg for rats and dogs, and mg for humans.

Table 3. Percentage of dose recovered after single oral administration of [^{14}C]Taselisib in rats, BDC rats, dogs, BDC dogs and humans (Arm B).

	Dose[a]	N	Gender	Collection period (h)	Percent dose recovered			
					Urine	Feces	Bile	Total
Rat	1	3	Male	0-192	5.58 (0.550)	94.2 (4.47)	NC	99.8 (4.27)
		3	Female	0-192	2.97 (0.294)	100 (2.42)	NC	103 (2.82)
Rat (BDC)	1	3	Male	0-168	17.6 (0.146)	NC	19.9 (2.97)	37.5 (3.11)
		3	Female	0-168	11.7 (2.22)	NC	22.5 (3.69)	34.3 (5.49)
Dog	2	2	Male	0-240	2.18 (NA)	94.1 (NA)	NC	96.3 (NA)
		2	Female	0-240	2.46 (NA)	96.1 (NA)	NC	98.6 (NA)
Dog (BDC)	2	2	Male	0-240	2.53 (NA)	28.2 (NA)	68.9 (NA)	96.3 (NA)
Human (Arm B)	3	6	Male	0-360	15.0 (3.59)	88.6 (8.23)	NC NC	104 (6.30)

Data are expressed as mean (SD); BDC: bile-duct cannulated; NA: Not applicable; NC: Not collected.
[a] Dose units are mg/kg for rats and dogs, and mg for humans.

Table 4. Distribution of radioactive Taselisib and its metabolites in urine, feces and/or bile from rats, dogs and humans after oral administration of [^{14}C]taselisib.

		Rat			Dog			Human	
Metabolite	Biotransformation	Urine	Feces	Bile (BDC)	Urine	Feces	Bile (BDC)	Urine	Feces
Taselisib	Parent	0.575	72.1	4.90	0.259	24.8	32.1	12.3	71.9
M1	Oxidation (+32 Da)	0.040	ND	0.995	ND	ND	ND	ND	ND
M2	Glutathione conjugation	ND	ND	0.550	ND	ND	ND	ND	ND
M3	Oxidation (+16 Da)	ND	ND	0.640	ND	ND	ND	ND	ND
M4	Oxidation & glucuronidation	ND	ND	0.760	ND	ND	ND	ND	ND
M5	Di-oxidation (+32 Da)	ND	2.74	0.260	ND	ND	ND	ND	2.65
M6	Oxidative ring opening	ND	ND	0.215	ND	ND	ND	ND	1.44
M7	Oxidation & sulfation	ND	ND	0.175	ND	ND	ND	ND	ND
M8	Oxidation (+16 Da)	0.100	ND	ND	ND	ND	ND	ND	ND
M9	Amide hydrolysis	ND	2.39	7.13	0.516	15.7	9.08	0.825	8.55
M10	Oxidation (+16 Da)	1.760	15.5	3.07	0.258	6.10	1.89	0.697	0.868
M11	Oxidation (+16 Da)	0.230	1.78	0.31	0.622	7.09	4.79	1.23	1.42
M12	Acetylation & ring opening	ND	ND	0.152	ND	ND	ND	ND	ND

M13	Oxidation & glucuronidation	D	D	D	ND	ND	ND	ND	ND
M14	Methylation & oxidation	ND	ND	ND	0.008	0.374	D	ND	ND
M15	Methylation & hydrolysis	ND	ND	ND	0.082	0.346	D	ND	ND
M16	Methylation & oxidation	ND	ND	ND	0.090	11.2	2.95	ND	ND
M17	Methylation	ND	ND	ND	0.222	29.5	18.1	ND	ND
% Dose subtotal		2.68	94.5	19.1	2.06	95.1	68.9	15.0	86.9
% Total excretion		4.27	97.1	21.2	2.32	95.1	68.9	15.0	88.5

D: Detected by mass spectrometry, ND; not detected
[a] Percentage of dose identified as a taselisib or metabolites

DMD Fast Forward. Published on January 9, 2023 as DOI: 10.1124/dmd.122.001096
This article has not been copyedited and formatted. The final version may differ from this version.

Legend for Figures

Figure 1. (A) Structure of Taselisib and position of radiolabeling, (B) study schemes of clinical studies (Arm A and Arm B). D; Day, Min; minimum.

Figure 2. (A) Plasma taselisib and [^{14}C]taselisib concentrations after oral administration of taselisib (3 mg) followed by iv administration of [^{14}C]taselisib (3 µg, 200 nCi) at 4h after oral administration of taselisib in humans (Arm A). (B) Blood and Plasma total radioactivity (TRA) and taselisib concentrations after oral administration of [^{14}C]taselisib (3 mg, 200 µCi) in humans (Arm B). TRA and taselisib concentrations in blood and plasma at 336 h in Arm B were below the limit of quantification. Data are expressed as mean±SD

Figure 3. Cumulative recovery of total radioactivity in urine, feces, and bile after oral administration of [^{14}C]taselisib in rats (1 mg/kg), dogs (2 mg/kg) and humans (3 mg). Data are expressed as mean±SD. Bile data from rats and dogs were collected from separate experiments using BDC animals.

Figure 4. Representative HPLC radiochromatograms in pooled plasma from rats, dogs and humans. cpm; count per minute, mins; minutes

Figure 5. Representative HPLC radiochromatograms in urine, feces and bile from rats after oral administration of [14C]Taselisib. cpm; count per minute, mins; minutes

Figure 6. Representative HPLC radiochromatograms in urine, feces and bile from dogs after oral administration of [^{14}C]Taselisib. cpm; count per minute, mins; minutes

Figure 7. Representative HPLC radiochromatograms in urine and feces from humans after oral administration of [^{14}C]Taselisib. cpm; count per minute, mins; minutes

Figure 8. (A) HMBC spectrum for M17 (500 MHz, CD_3OD) and (B) key HMBC correlations of M17.

Figure 9. Characterization of methyltransferases involved in M17 formation in dogs. (A) Taselisib was incubated with human, mouse, rat, dog and monkey hepatocytes for 3 h. Extracted ion chromatogram of M17 and taselisib was presented. (B) Taselisib was incubated with dog liver microsome (DLM) and dog liver cytosol (DLC). Extracted ion chromatogram of M17 and taselisib was presented. (C) Taselisib was incubated with dog hepatocytes in the presence of various methyltransferase inhibitors for 3 hours: CTL; DMSO vehicle control, Amo; amodiaquine (HNMT inhibitor), DCMB; 2,3-dichloromethylbenzylamine hydrochloride (TMT inhibitor), Met; 1-methyl nicotinamide (NNMT inhibitor), Sul; sulfasalazine (TPMT inhibitor), Tol; tolcapone (COMT inhibitor). *; $p<0.05$ compared to CTL from student t-test.

Figure 10. Proposed disposition of taselisib after oral administration in humans

DMD Fast Forward. Published on January 9, 2023 as DOI: 10.1124/dmd.122.001096
This article has not been copyedited and formatted. The final version may differ from this version.

Figure 11. Proposed major metabolic pathways of taselisib in rats (R), dogs (D) and humans (H)

(A)

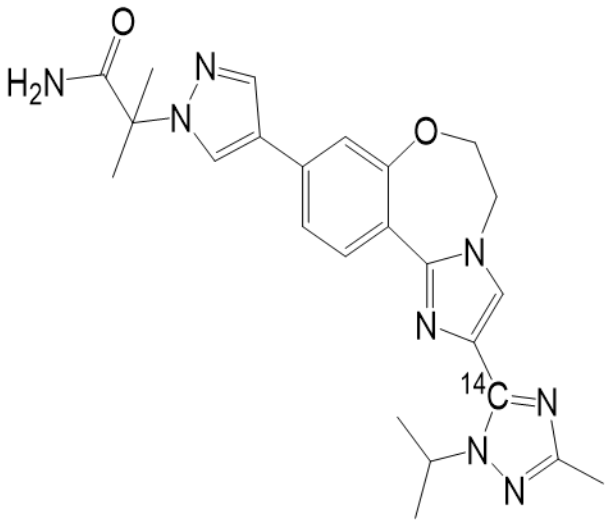

Taselisib

(B)

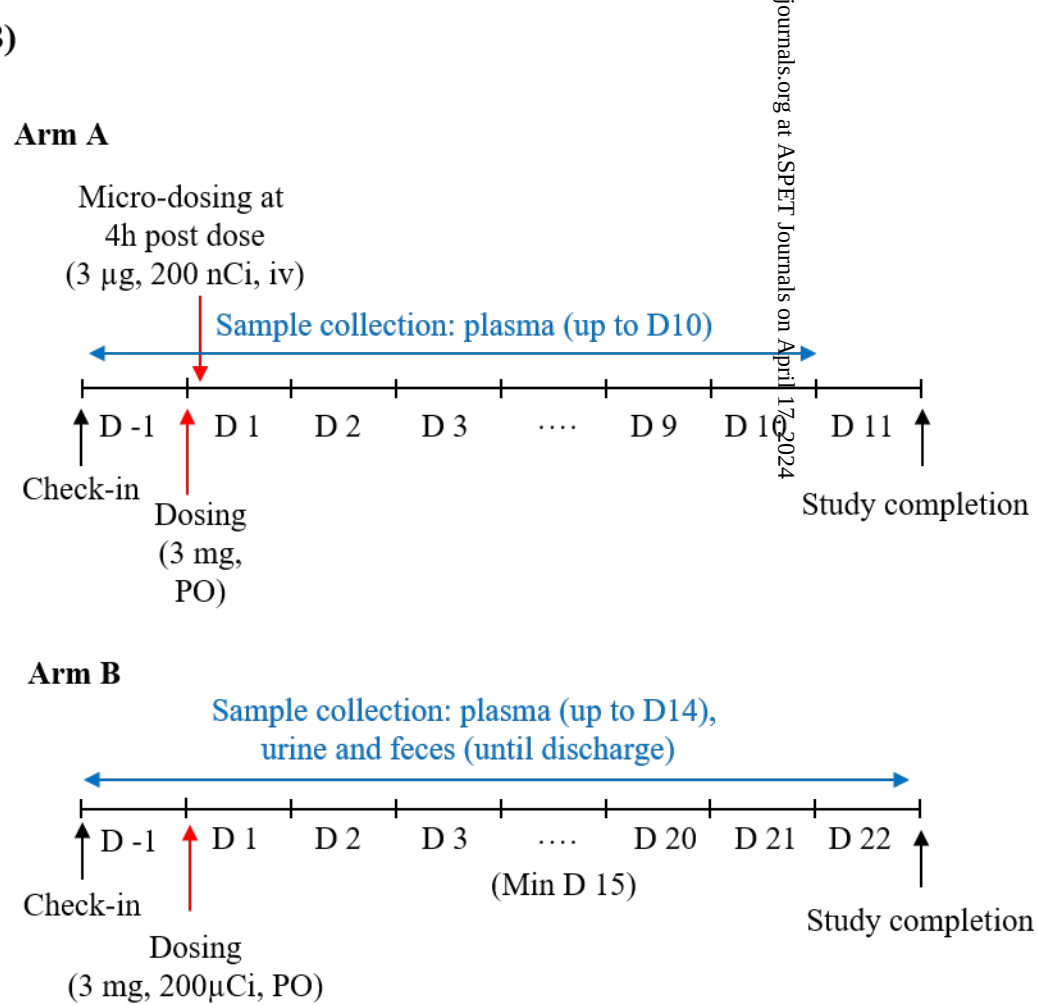

Figure 1

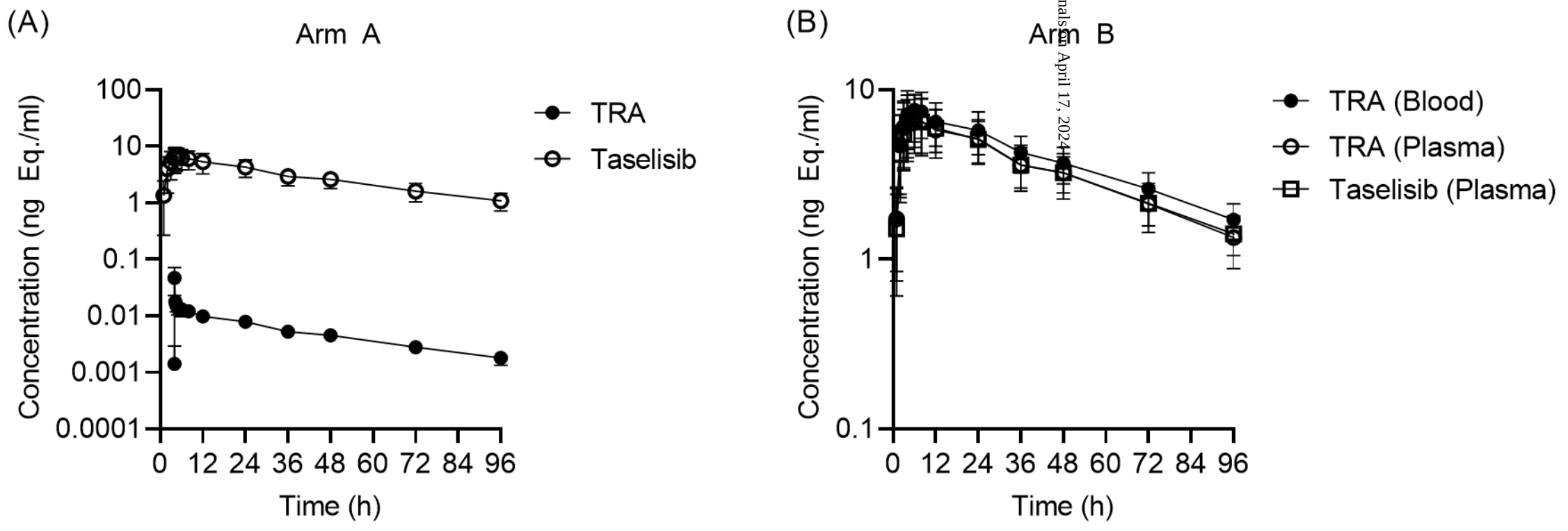

Figure 2

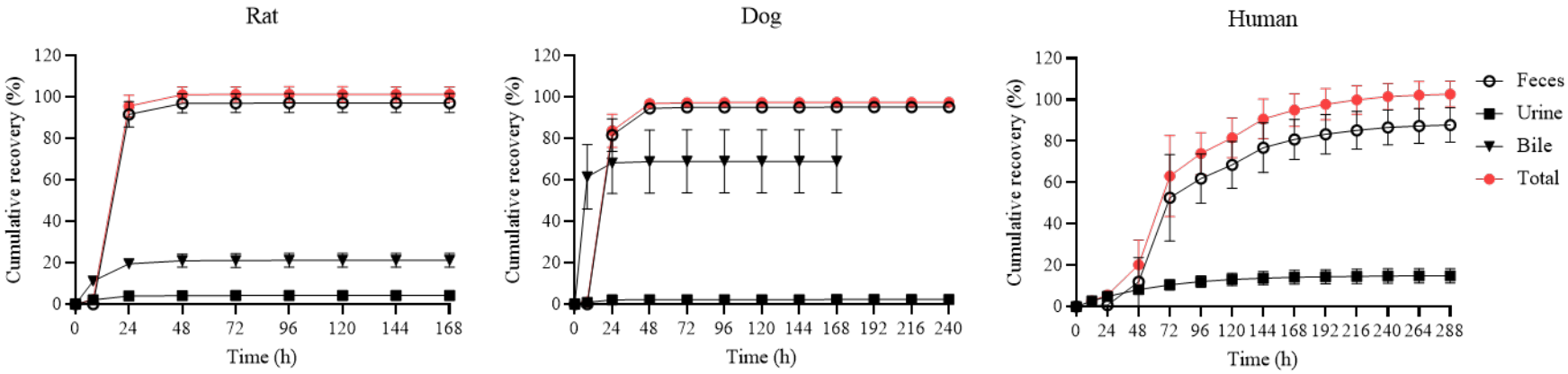
Rat
Dog
Human
Cumulative recovery (%)
Time (h)
Feces
Urine
Bile
Total

Figure 3

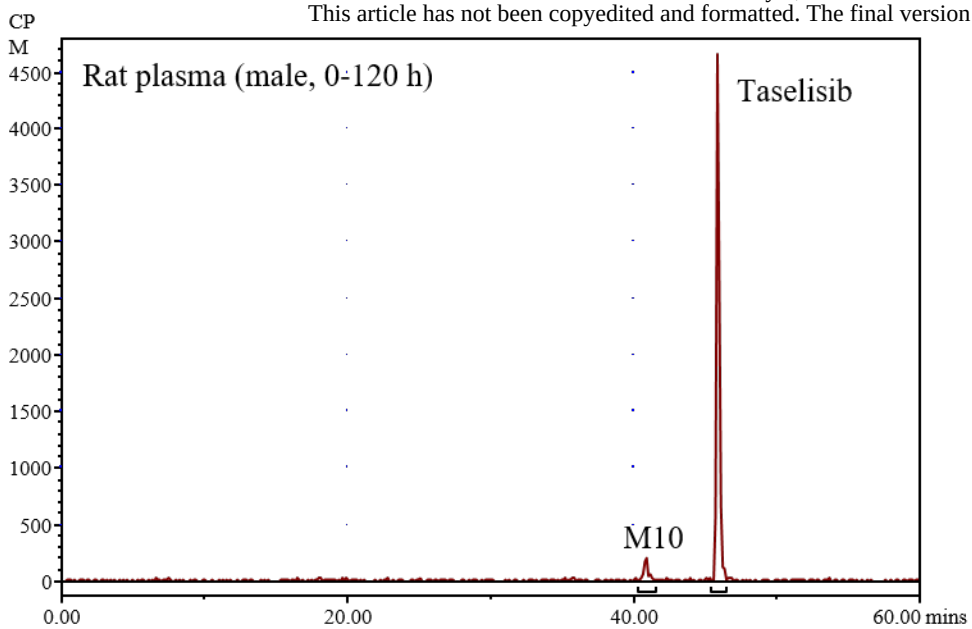

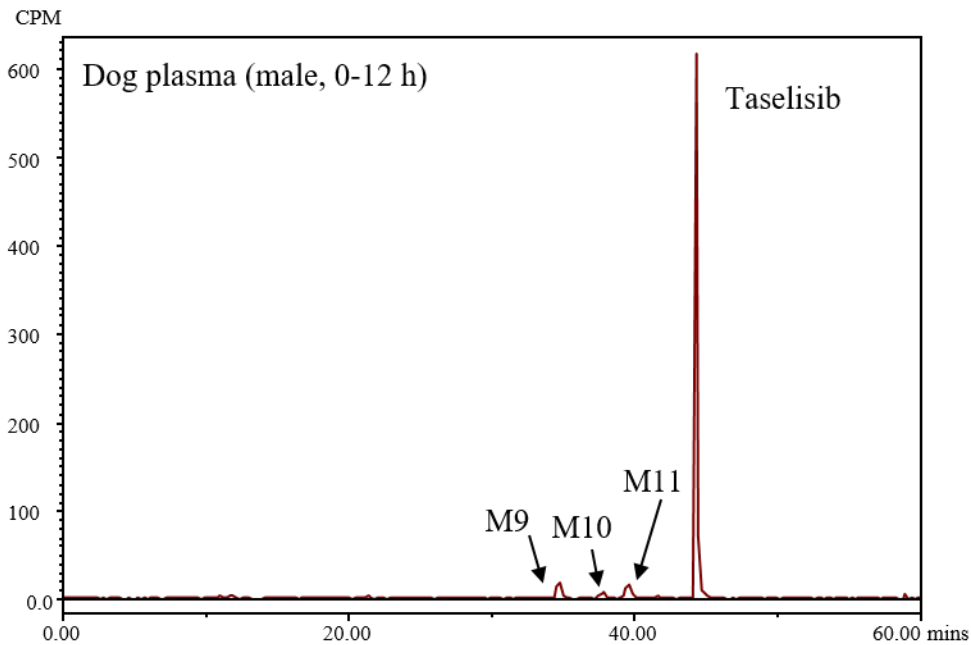

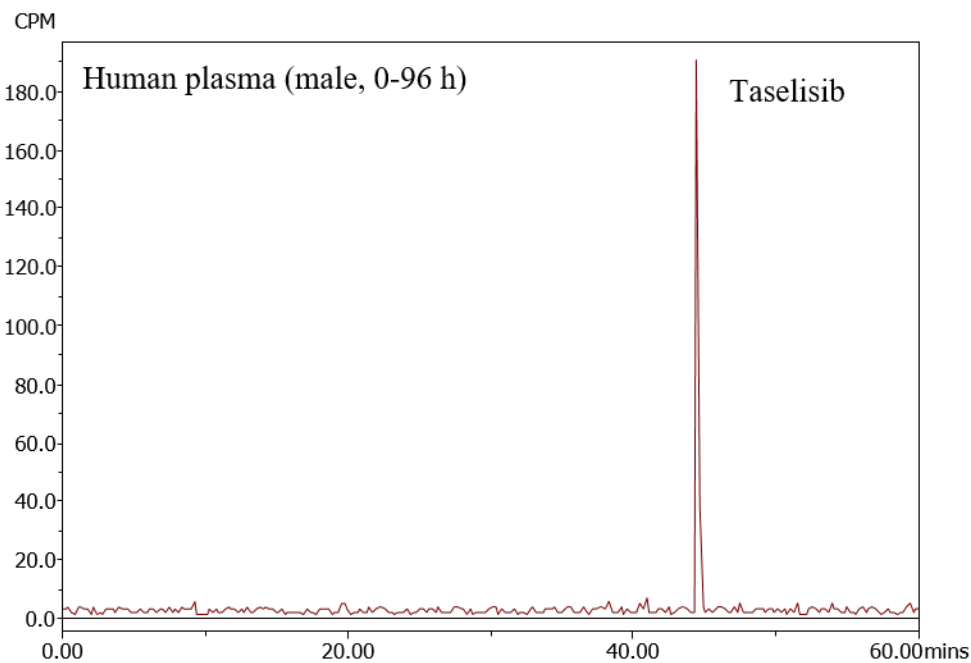

Figure 4

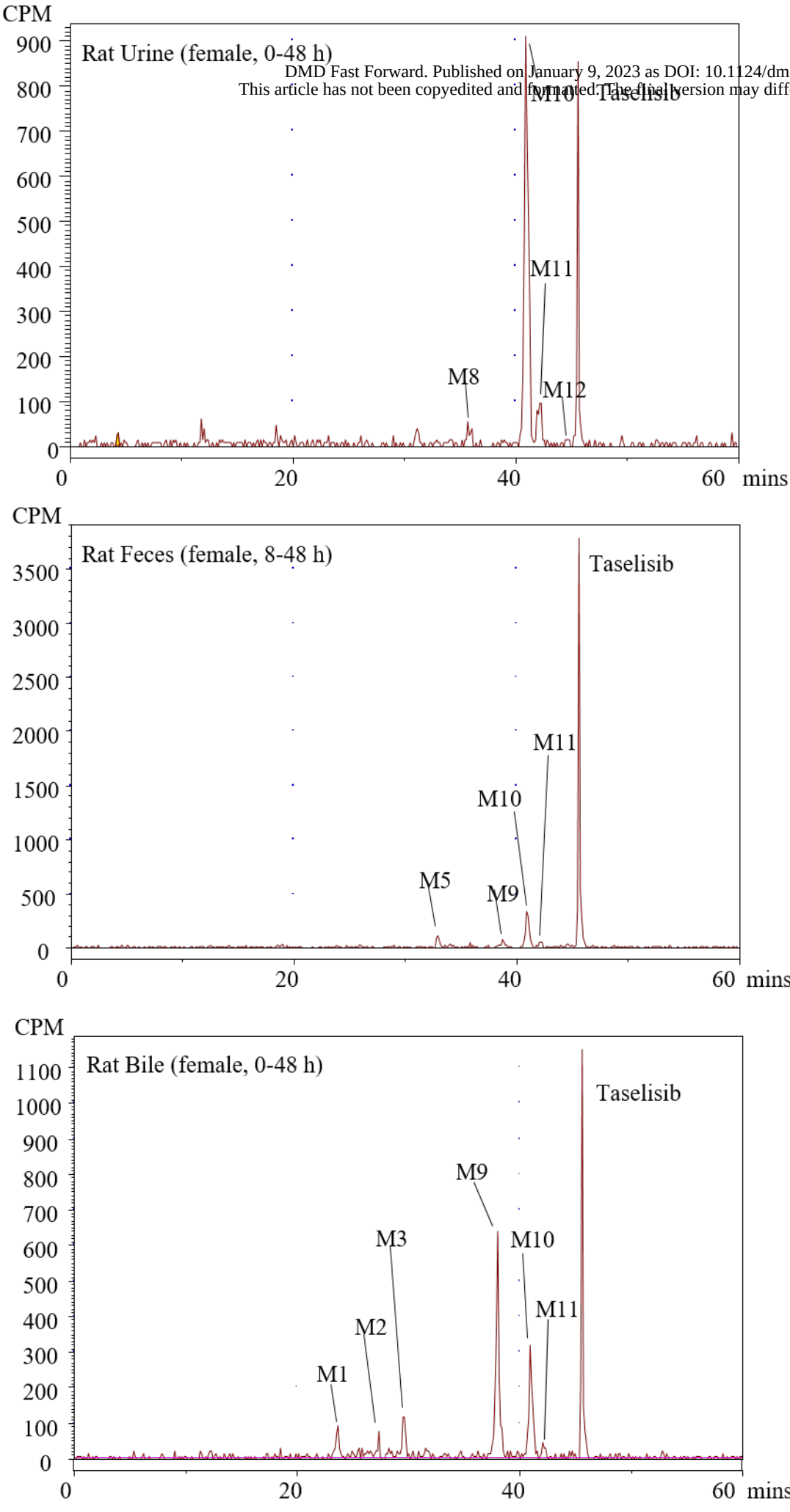

Figure 5

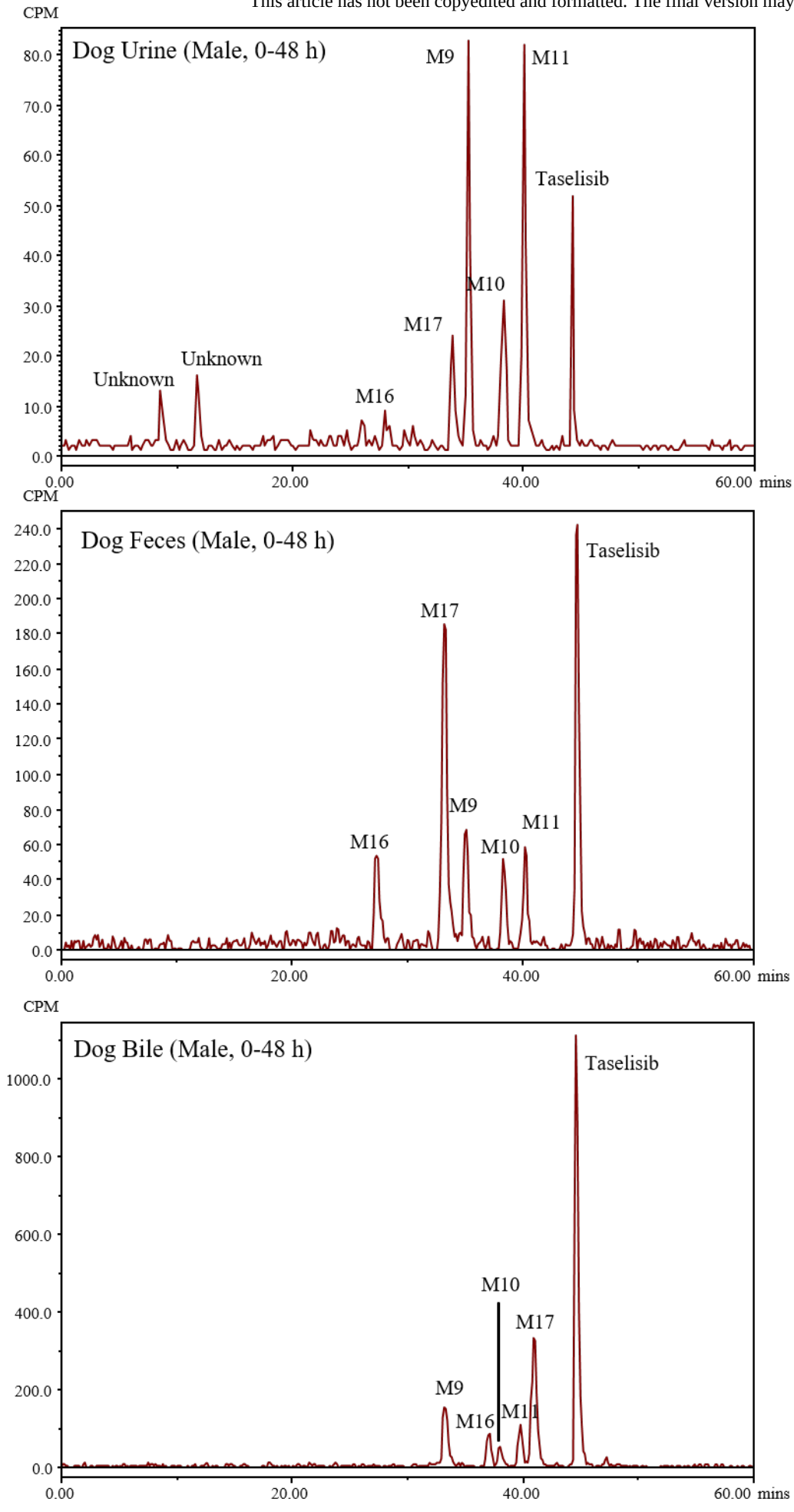

Figure 6

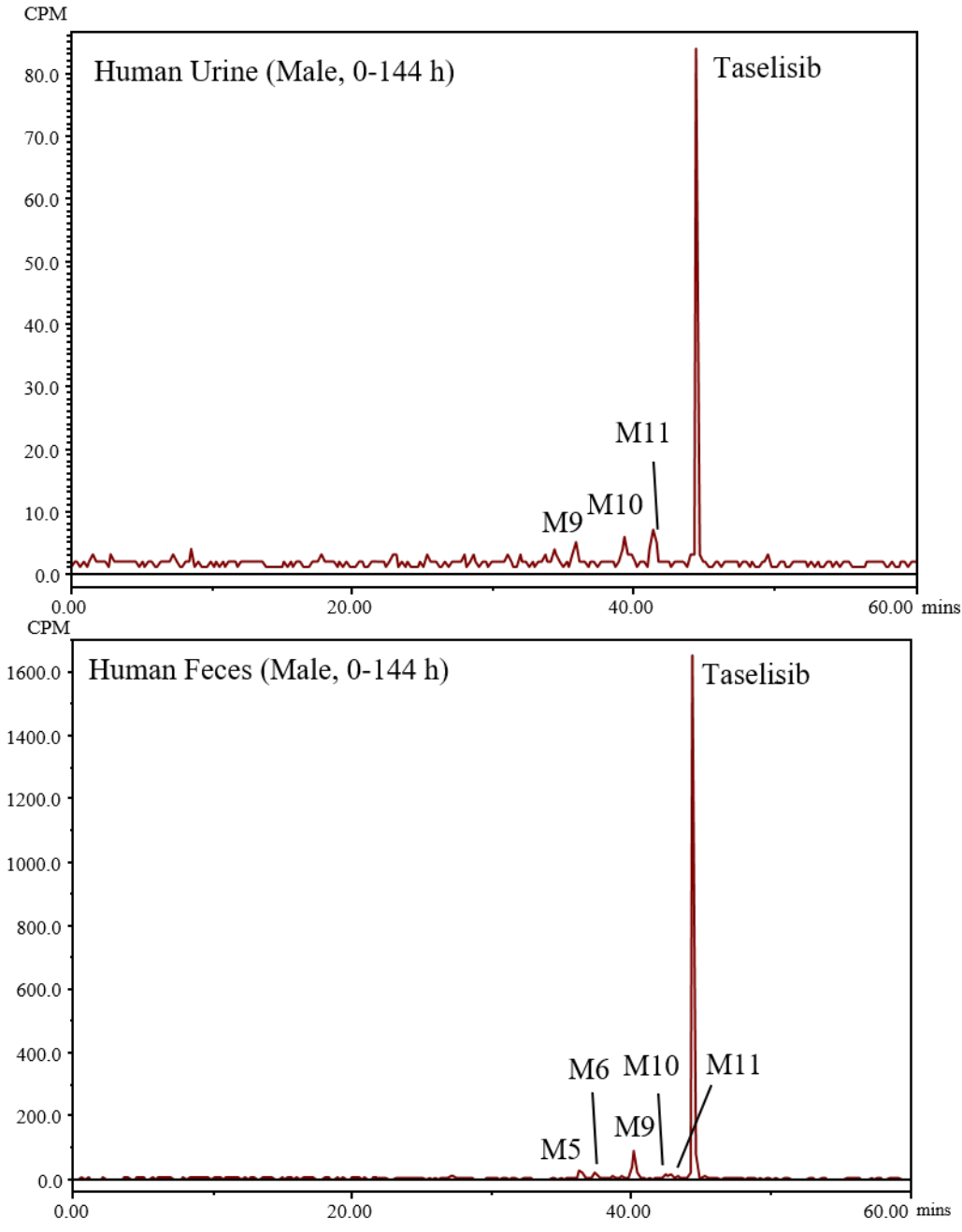
CPM
Human Urine (Male, 0-144 h)
Taselisib
M11
M10
M9
80.0
70.0
60.0
50.0
40.0
30.0
20.0
10.0
0.0
0.00
20.00
40.00
60.00 mins
CPM
Human Feces (Male, 0-144 h)
Taselisib
M6
M10
M11
M9
M5
1600.0
1400.0
1200.0
1000.0
800.0
600.0
400.0
200.0
0.0
0.00
20.00
40.00
60.00 mins

Figure 7

(A)

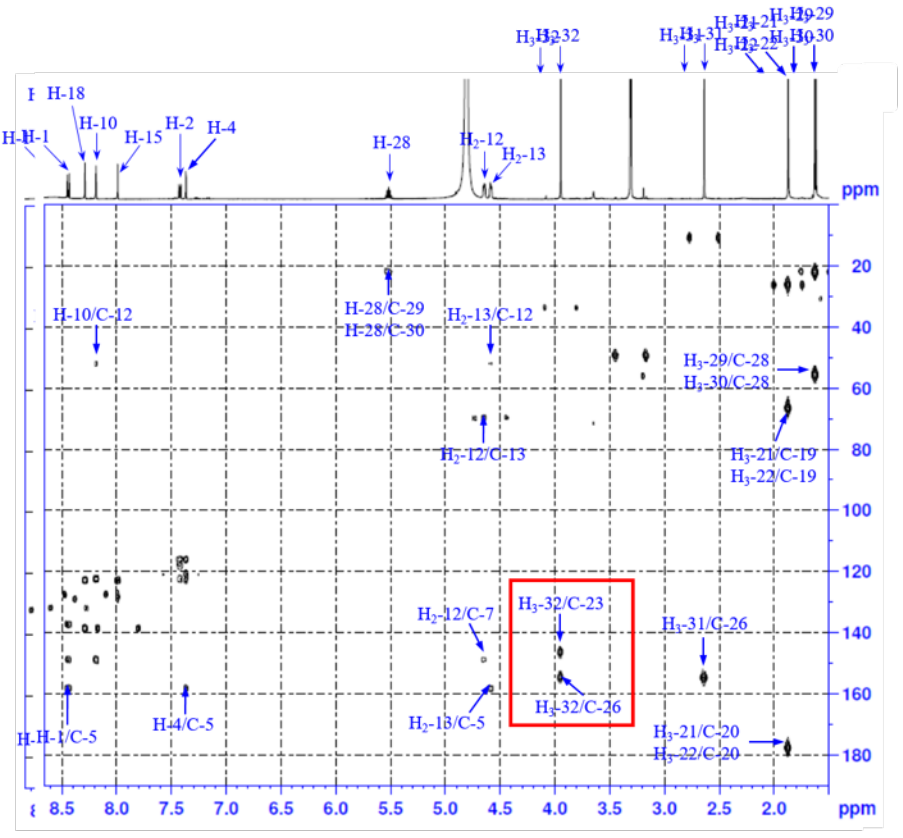
H-18
H-10
H-15
H-2
H-4
H-1
H-28
H2-12
H2-13
H3-32
H3-31
H3-21
H3-22
H3-29
H3-30
ppm
H-10/C-12
H-28/C-29
H-28/C-30
H2-13/C-12
H3-29/C-28
H3-30/C-28
H2-12/C-13
H3-21/C-19
H3-22/C-19
H2-12/C-7
H3-32/C-23
H3-31/C-26
H-1/C-5
H-4/C-5
H2-13/C-5
H3-32/C-26
H3-21/C-20
H3-22/C-20
8.5
8.0
7.5
7.0
6.5
6.0
5.5
5.0
4.5
4.0
3.5
3.0
2.5
2.0
ppm

(B)

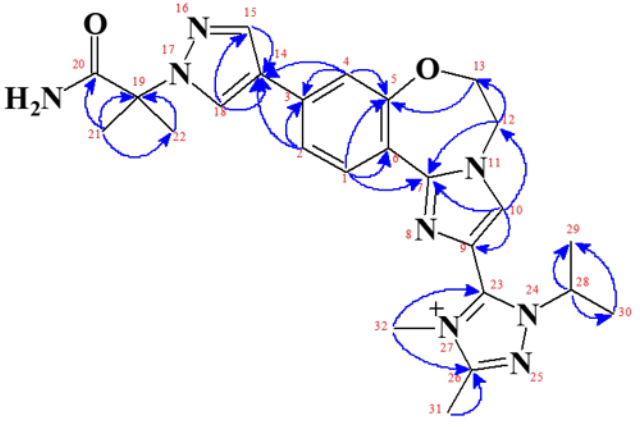
O
H2N
N
N
O
N
N
N
+
N
N

Figure 8

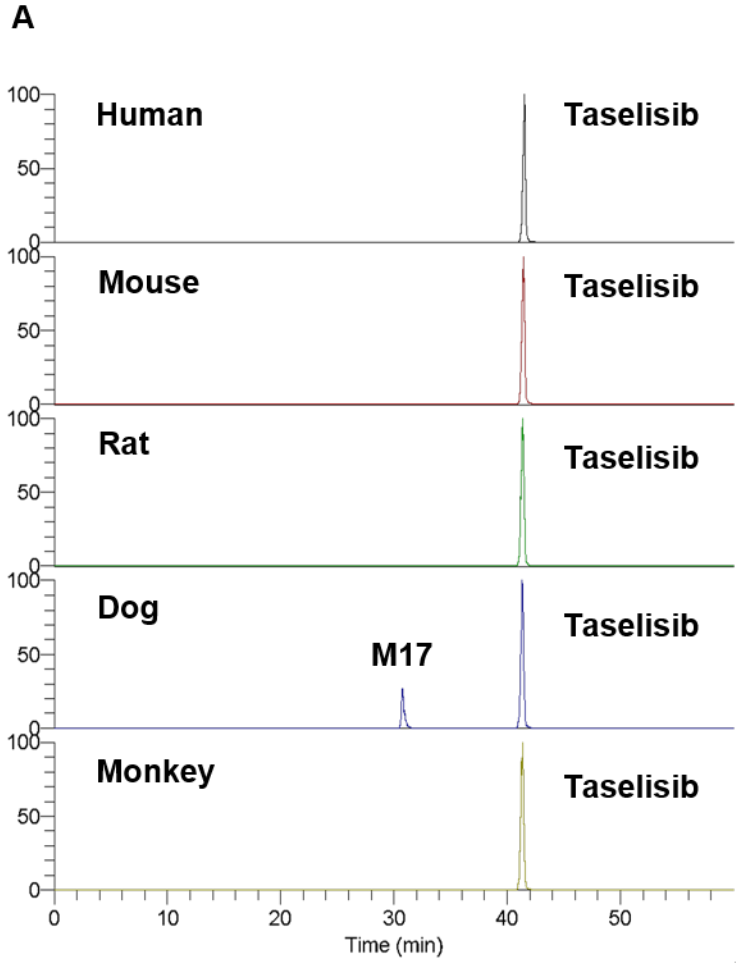

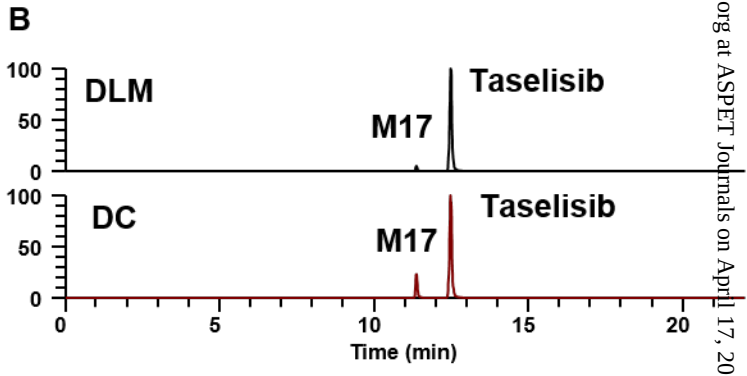

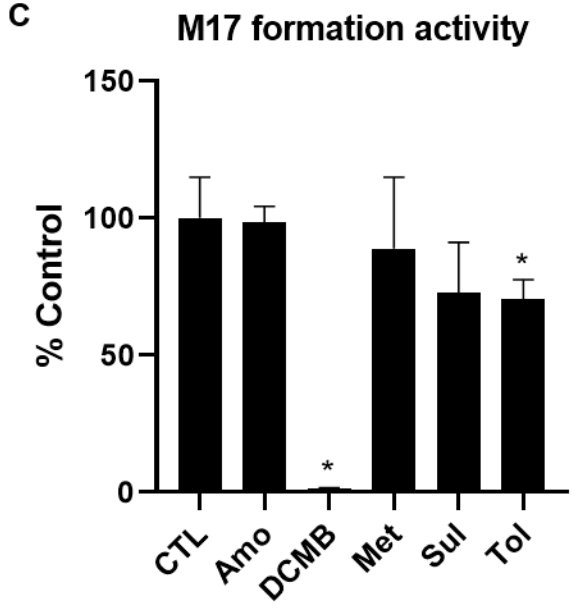

Figure 9

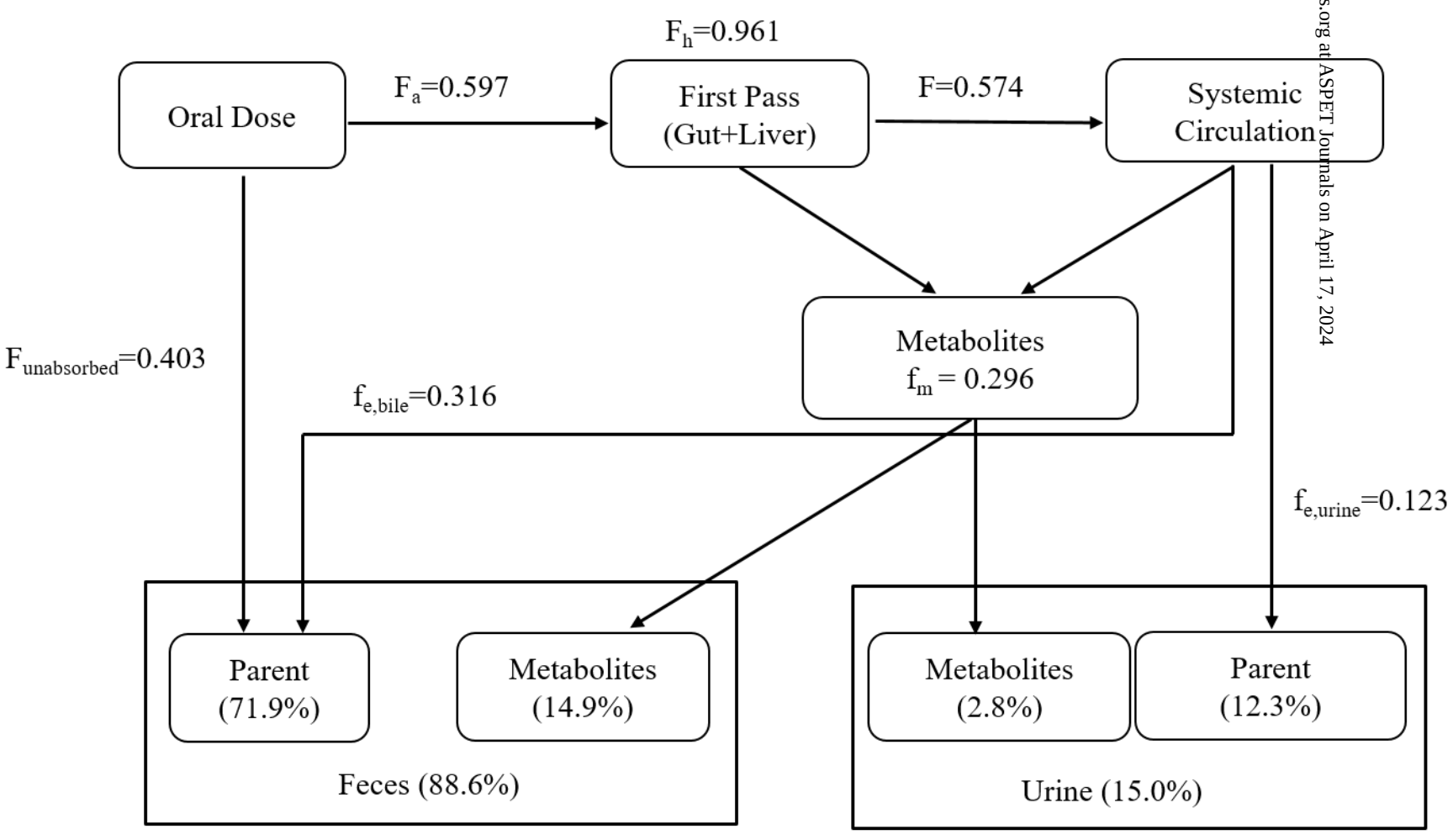

Figure 10

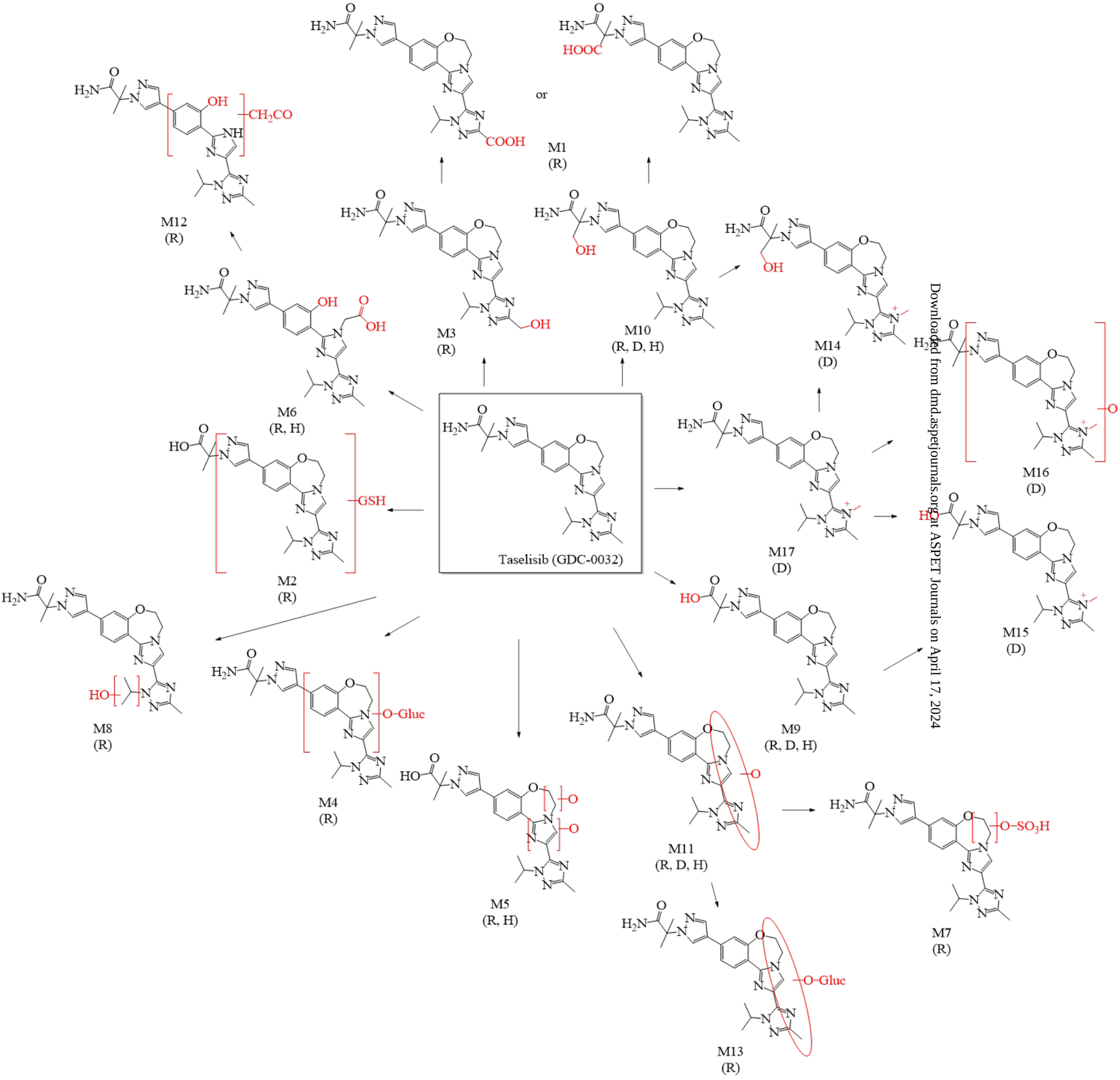

Figure 11

Drug Metabolism and Disposition

DMD-AR-2022-001096

Supplementary data

Absorption, Metabolism, and Excretion of Taselisib (GDC-0032), a Potent β-sparing PI3K Inhibitor, in Rats, Dogs, and Humans

Shuguang Ma[*, 1], Sungjoon Cho*, Srikumar Sahasranaman[2], Weiping Zhao, Jodie Pang, Xiao Ding, Brian Dean, Bin Wang[3], Jerry Y. Hsu[4], Joseph Ware[5], Laurent Salphati

Department of Drug Metabolism and Pharmacokinetics (SM, SC, WZ, JP, XD, BD, LS) and Department of Clinical Pharmacology (SS, JH, JW), Genentech, Inc., 1 DNA Way, South San Francisco, CA, 94080; XenoBiotic Laboratories (BW), Inc., 107 Morgan Lane, Plainsboro, NJ 08536

* Contributed equally

[1]Current affiliation: Pharmacokinetics and Drug Metabolism, Amgen, Inc., South San Francisco, CA

[2] Current affiliation: Clinical Pharmacology, BeiGene, San Mateo, CA

[3] Current affiliation: Ingredient Research, The Coca-Cola Company, Atlanta, GA

[4] Current affiliation: Clinical Development, ArriVent Biopharma, Burlingame, CA

[5] Current affiliation: Clinical Pharmacology, Seagen, South San Francisco, CA

Corresponding author:

Laurent Salphati, Pharm.D., Ph.D.

Drug Metabolism and Pharmacokinetics, Genentech, Inc., 1 DNA Way, South San Francisco, CA 94080. Phone: 650-467-1796. Email: salphati.laurent@gene.com

Supplementary Table S1. Summary of structures and mass fragmentation for metabolites of Taselisib in rats, dogs and humans.

Analyte	Observed MH+ (Chemical formula	Source	Structure
Taselisib	461.2408 ($C_{24}H_{29}N_8O_2^+$)	Rat: P, U, F, B Dog: P, U, F, B Human: P, U, F	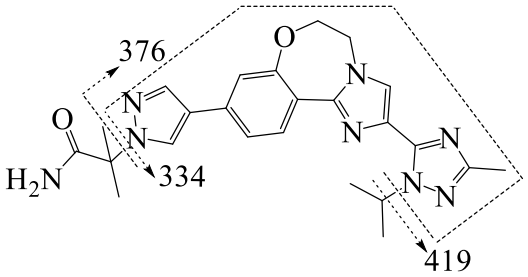
M1 (Oxidation to carboxylic acid)	*493.2182 ($^{14}CC_{23}H_{27}N_8O_4^+$)	Rat: B	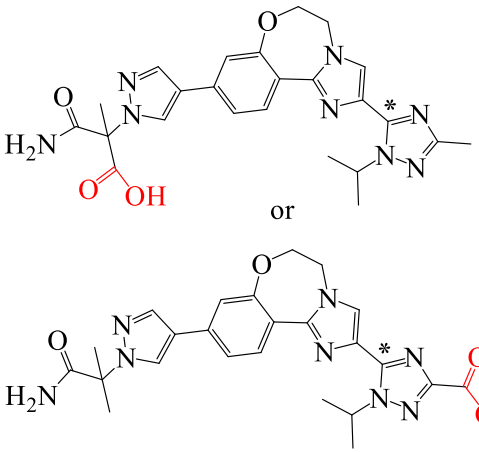 $[M+H]^+$=493 491-H_2O= 473 493-CO_2=449 449-NH_3=432 449-C_3H_6=407 432-CO=404 449-NH_3-C_3H_6=39
M2 (Glutathione conjugation	*768.3123 ($^{14}CC_{33}H_{44}N_{11}O_8S^+$)	Rat: B	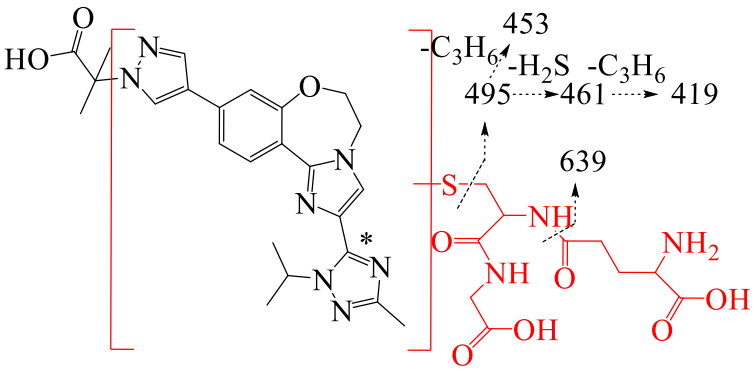

Supplementary Table S1 (continued). Summary of structures and mass fragmentation for metabolites of Taselisib in rats, dogs and humans.

Analyte	Observed MH+ (Chemical formula	Source	Structure
M3 (oxidation)	*479.2389 ($^{14}CC_{23}H_{29}N_8O_3^+$)	Rat: B	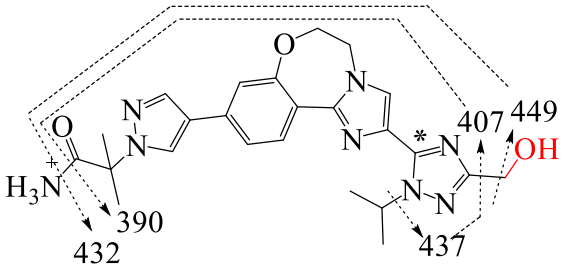
M4 (oxidation & glucuronidation)	*655.2713 ($^{14}CC_{29}H_{37}N_8O_9^+$)	Rat: B	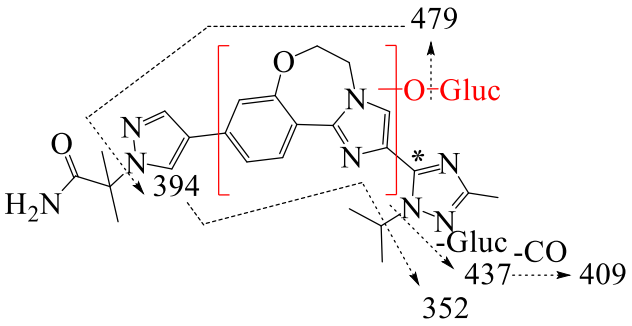
M5 (Di-oxidation)	493.2306 ($C_{24}H_{29}N_8O_4^+$)	Rat: F, B Human: F	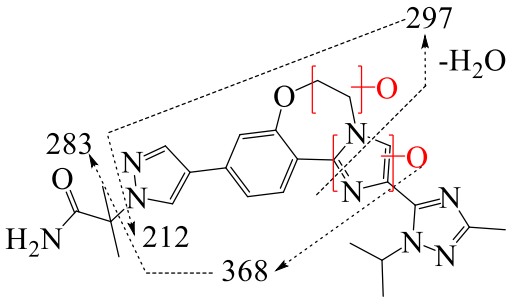
M6 (Oxidative ring opening)	493.2306 ($C_{24}H_{29}N_8O_4^+$)	Rat: B Human: F	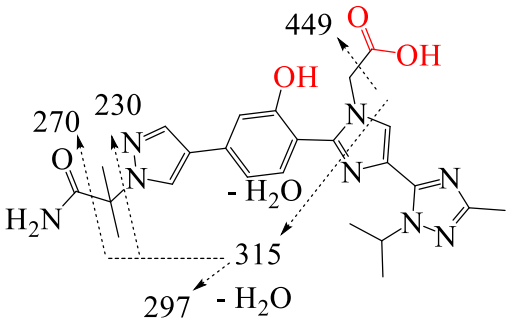

Supplementary Table S1. Summary of structures and mass fragmentation for metabolites of Taselisib in rats, dogs and humans.

Analyte	Observed MH+ (Chemical formula	Source	Structure
M7 (Oxidation & sulfation)	*559.1958 ($^{14}CC_{23}H_{29}N_8O_6S^+$)	Rat: B	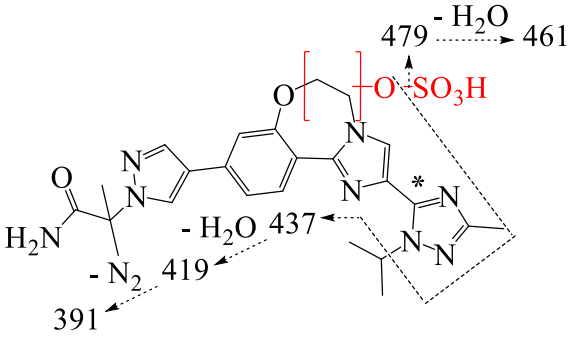
M8 (Oxidation)	*479.2390 ($^{14}CC_{23}H_{29}N_8O_3^+$)	Rat: U	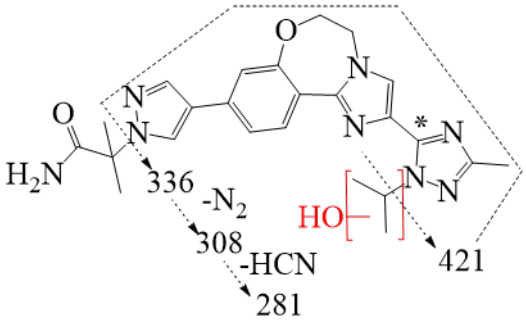
M9 (Amide hydrolysis)	*462.2248 ($C_{24}H_{28}N_7O_3^+$)	Rat: F, B Dog: P, U, F, B Human: U, F	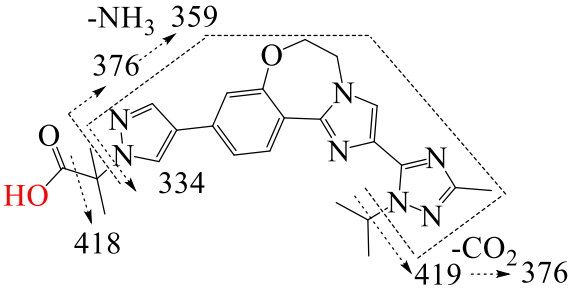
M10 (Oxidation)	477.2370 ($C_{24}H_{29}N_8O_3^+$)	Rat: P, U, F, B Dog: P, U, F, B Human: U, F	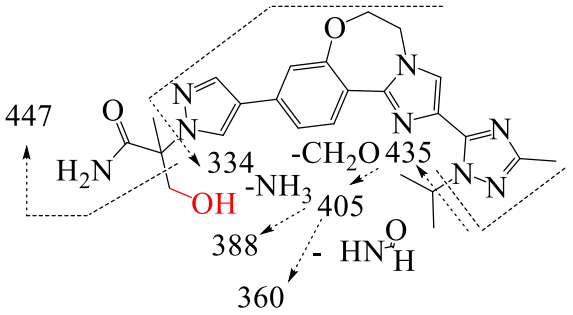

Supplementary Table S1 (continued). Summary of structures and mass fragmentation for metabolites of Taselisib in rats, dogs and humans.

Analyte	Observed MH+ (Chemical formula	Source	Structure
M11 (Oxidation)	477.2359 ($C_{24}H_{29}N_8O_3^+$)	Rat: U, F, B Dog: P, U, F, B Human: U, F	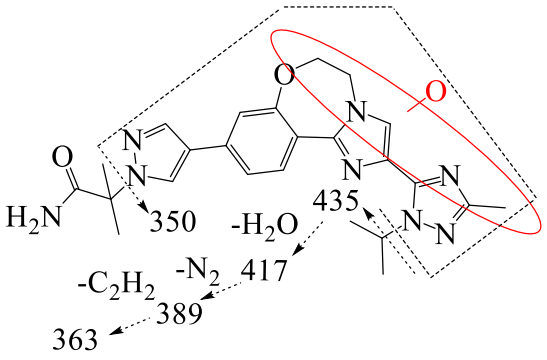
M12 (Acetylation & ring opening)	*479.2392 ($^{14}CC_{23}H_{29}N_8O_3^+$)	Rat: B	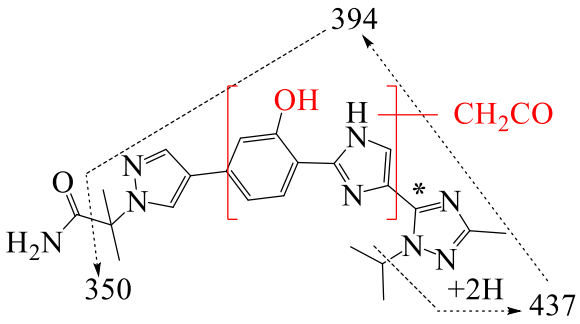
M13 (Oxidation & glucuronidation)	*655.2710 ($^{14}CC_{29}H_{37}N_8O_9^+$)	Rat: U, F, B	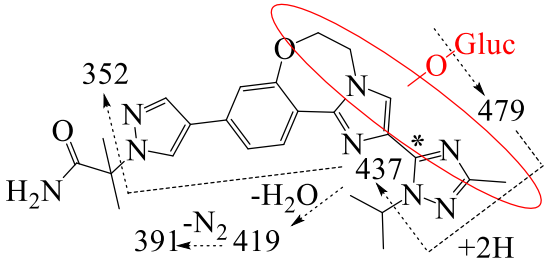
M14 (Methylation & Oxidation)	491.2526 ($C_{25}H_{31}N_8O_3^+$)	Dog: P, U, F, B	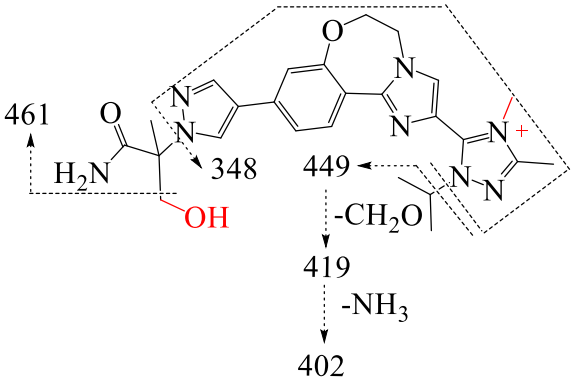

Supplementary Table S1 (continued). Summary of structures and mass fragmentation for metabolites of Taselisib in rats, dogs and humans.

Analyte	Observed MH+ (Chemical formula	Source	Structure
M15 (Methylation & hydrolysis)	476.2416 ($C_{25}H_{30}N_7O_3^+$)	Dog: P, U, F, B	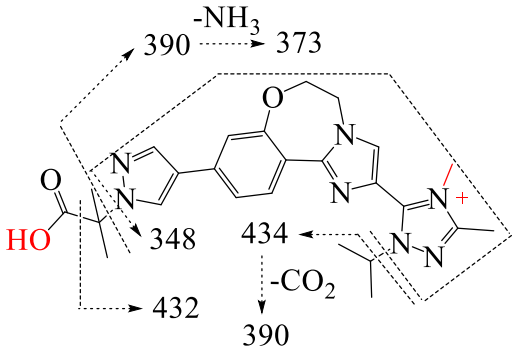
M16 (Methylation & oxidation)	491.2525 ($C_{25}H_{31}N_8O_3^+$)	Dog: P, U, F, B	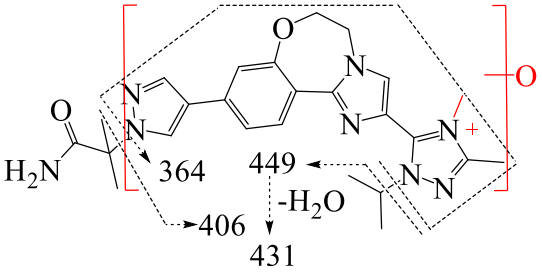
M17 (Methylation)	475.2571 ($C_{25}H_{31}N_8O_2^+$)	Dog: P, U, F, B	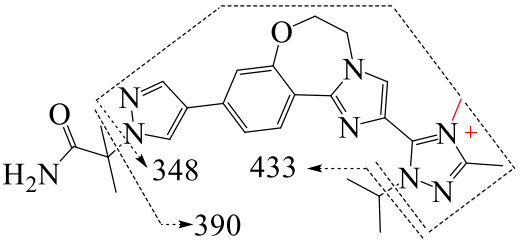

*; **m/z values of an analyte and its fragments were based on [^{14}C] compounds.**

Supplementary Table S2. ^{1}H and ^{13}C NMR Data for GDC-0032 and M17 (δ in ppm)

Position	GDC-0032[a]		M17[a]	
	^{13}C	^{1}H, multiplicity (J in Hz)	^{13}C	^{1}H, multiplicity (J in Hz)
1	131.8	8.41, d (8.4)	131.8	8.43, d (8.4)
2	121.0	7.37, dd (1.8,8.4)	120.8	7.41, dd (1.8,8.4)
3	117.3	---	116.2	---
4	118.1	7.30, d (1.8)	118.0	7.36, d (1.8)
5	158.0	---	158.3	---
6	136.4	---	137.1	---
7	146.8	---	148.8	---
9	131.3	---	122.2	---
10	124.8	7.71, s	128.9	8.19, s
12	51.5	4.52, m	51.7	4.64, m
13	70.0	4.52, m	69.5	4.59, m
14	123.2	---	122.8	---
15	138.8	7.97, brs	138.6	7.99, brs
18	127.5	8.27, d (0.5)	127.3	8.29, d (0.5)
19	66.6	---	66.2	---
20	177.9	---	177.7	---
21	26.4	1.86, s	26.0	1.87, s
22	26.4	1.86, s	26.0	1.87, s
23	149.5	---	146.4	---
26	160.3	---	154.7	---
28	52.4	5.91, sep (6.6)	55.4	5.52, sep (6.6)
29	22.7	1.54, d (6.6)	21.8	1.62, d (6.6)
30	22.7	1.54, d (6.6)	21.8	1.62, d (6.6)
31	13.7	2.36, s	10.6	2.64, s
32			33.6	3.95, s

[a] Measured in methanol-d_4 with ^{1}H at 500 MHz, and ^{13}C at 125 MHz. The ^{13}C NMR signals for M17 were indirect from HSQC and/or HMBC spectra.

d: doublet; dd: double doublet; s: singlet; brs: broad singlet; sep: septet; m: multiplet.

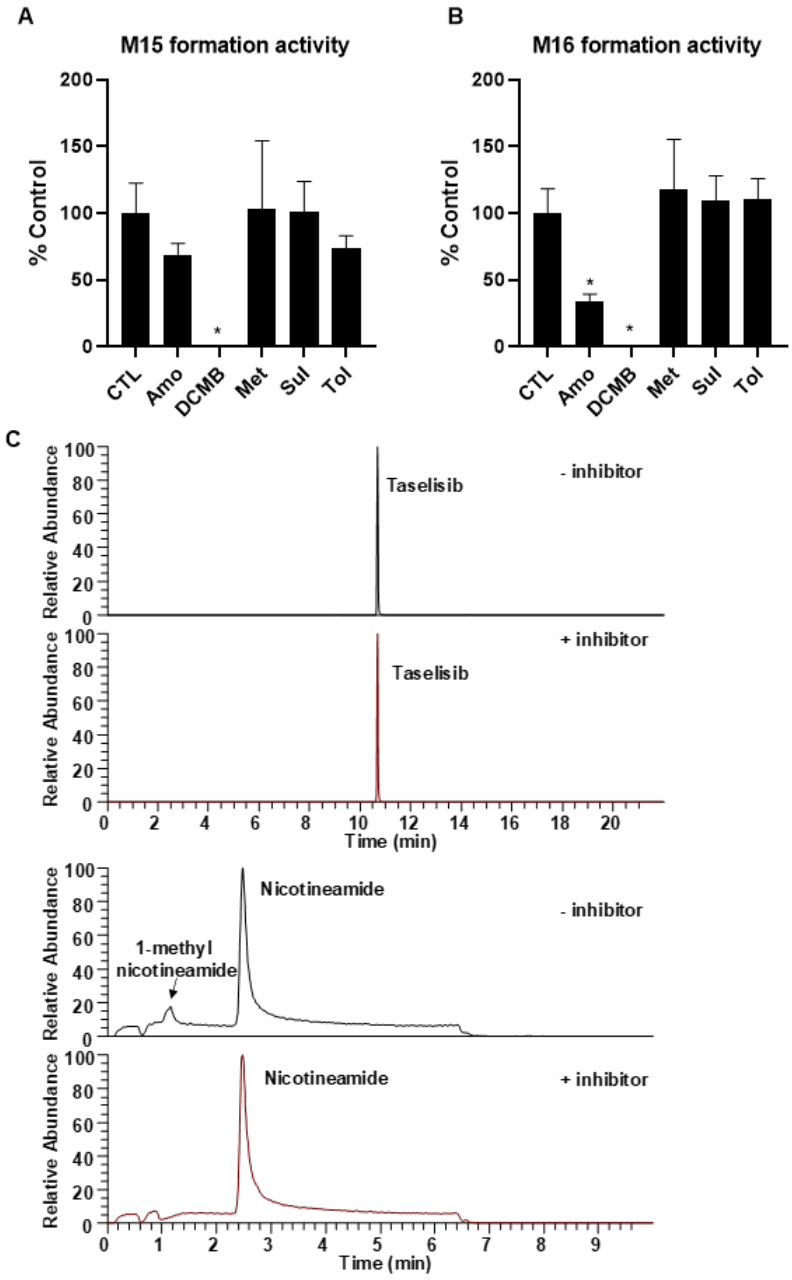

Supplementary Figure S1. Chracterization of methyltransferase involved in inavolisib metabolism in dogs. (A & B) Taselisib was incubated with dog hepatocytes in the presence of various human methyltransferase inhibitors for 3 h: Amo; amodiaquine (HNMT inhibitor), DCMB; 2,3-dichloromethylbenzylamine (TMT inhibitor), Met; 1-methyl nicotinamide (NNMT inhibitor), Sul; sulfasalazine (TPMT inhibitor), Tol; tolcapone (COMT inhibitor). (C) Recombinant NNMT was incubated with taselisib or nicotine amide for 1 hours in the presence of 5-amino-1-methylquinolin-1-ium iodide (NNMT inhibitor). *; $p<0.05$ compared to CTL from student t-test.